Retrolinkin recruits the WAVE1 protein complex to facilitate BDNF-induced TrkB endocytosis and dendrite outgrowth

Chenchang Xu[a,b,c], Xiuping Fu[a,c,†], Shaoxia Zhu[a,b], and Jia-Jia Liu[a,b,*]
[a]State Key Laboratory of Molecular Developmental Biology, Institute of Genetics and Developmental Biology, and [b]CAS Center for Excellence in Brain Science and Intelligence Technology, Chinese Academy of Sciences, Beijing 100101, China; [c]Graduate School, University of Chinese Academy of Sciences, Beijing 100039, China

ABSTRACT **Retrolinkin, a neuronal membrane protein, coordinates with endophilin A1 and mediates early endocytic trafficking and signal transduction of the ligand–receptor complex formed between brain-derived neurotrophic factor (BDNF) and its receptor, tropomyosin-related kinase B (TrkB), in dendrites of CNS neurons. Here we report that retrolinkin interacts with the CYFIP1/2 subunit of the WAVE1 complex, a member of the WASP/WAVE family of nucleation-promoting factors that binds and activates the Arp2/3 complex to promote branched actin polymerization. WAVE1, not N-WASP, is required for BDNF-induced TrkB endocytosis and dendrite outgrowth. Disruption of the interaction between retrolinkin and CYFIP1/2 impairs recruitment of WAVE1 to neuronal plasma membrane upon BDNF addition and blocks internalization of activated TrkB. We also show that WAVE1-mediated endocytosis of BDNF-activated TrkB is actin dependent and clathrin independent. These results not only reveal the mechanistic role of retrolinkin in BDNF–TrkB endocytosis, but also indicate that WASP/WAVE-dependent actin polymerization during endocytosis is regulated by cell type–specific and cargo-specific modulators.**

Monitoring Editor
Jean E. Gruenberg
University of Geneva

Received: May 25, 2016
Revised: Aug 29, 2016
Accepted: Aug 31, 2016

INTRODUCTION

Brain-derived neurotrophic factor (BDNF) is a member of the neurotrophin (NT) family, which includes nerve growth factor (NGF), NT-3, and NT-4/5. It binds and activates the cell surface receptor tropomyosin-related kinase B (TrkB), a receptor tyrosine kinase, to regulate neuronal development, survival, and function in the CNS (Huang and Reichardt, 2003; Segal, 2003). Binding of BDNF triggers TrkB dimerization and autophosphorylation/activation of its intracellular domain, which provides docking sites for adaptor and effector proteins to activate multiple signaling pathways (Huang and Reichardt, 2003; Segal, 2003). In the highly polarized neuronal cell, the NT ligand–receptor complex is internalized through receptor-mediated endocytosis and transported from the nerve terminal to the cell body in the form of signaling endosomes (Howe *et al.*, 2001; Delcroix *et al.*, 2003; Valdez *et al.*, 2005; Harrington *et al.*, 2011; Cosker and Segal, 2014). Like those of other NTs and their cognate receptors, the endocytic trafficking of BDNF–TrkB is a complex and highly regulated process that endows the spatiotemporal specificity of downstream signaling events (Chen *et al.*, 2005; Zheng *et al.*, 2008; Fu *et al.*, 2011). However, the molecular mechanisms underlying BDNF–TrkB trafficking remain largely unknown.

The Wiskott–Aldrich syndrome protein (WASP)/verprolin homologue (WAVE) family of nucleation-promoting factors (NPFs) activates the actin-related protein 2/3 (Arp2/3) complex—the actin nucleation factor—to induce actin polymerization during multiple cellular processes, including cell migration, axonal outgrowth, dendritic spine morphogenesis, and synapse formation (Derivery and Gautreau, 2010). The WASP/WAVE family consists of WASP, N-WASP, WAVE1, WAVE2, and WAVE3 (WASP-family verprolin-homologous proteins), characterized by a C-terminal VCA domain that binds to both Arp2/3 and actin to provide the nucleation reaction with monomeric actin (G-actin) when Arp2/3 initiates a branch from preexisting actin filaments (Derivery and Gautreau, 2010).

This article was published online ahead of print in MBoC in Press (http://www.molbiolcell.org/cgi/doi/10.1091/mbc.E16-05-0326) on September 7, 2016.

†Present address: Solomon H. Snyder Department of Neuroscience, Johns Hopkins School of Medicine, Baltimore, MD 21205.

*Address correspondence to: Jia-Jia Liu (jjliu@genetics.ac.cn).

Abbreviations used: DIV, days in vitro; VCA, verprolin, cofilin, and acidic.

Among them, N-WASP plays a regulatory role in actin-based vesicular transport and endocytosis of the epidermal growth factor receptor (EGFR) and transferrin (Tf) receptor in fibroblasts (Kessels and Qualmann, 2002; Innocenti *et al.*, 2005). N-WASP and Arp2/3 are recruited to sites of clathrin-mediated endocytosis (CME; Merrifield *et al.*, 2004), and N-WASP deficiency causes a reduction in both recruitment of actin and Arp2/3 to clathrin-coated pits and receptor-mediated endocytosis of EGF (Benesch *et al.*, 2005). It was later found that N-WASP interacts with SNX9 and functions in both clathrin-mediated and clathrin–independent, actin-dependent fluid-phase endocytosis (Shin *et al.*, 2007; Yarar *et al.*, 2007).

Unlike N-WASP, of which the VCA domain is masked by intramolecular interaction, WAVE associates with other proteins to form a heteropentameric complex called WAVE regulatory complex (WRC), which is composed of WAVE, Nck-associated protein 1 (NAP1 or Nckap1), Sra1/PIR121 (also known as cytoplasmic FMR1-interactiing protein 1/2, [CYFIP1/CYFIP2]), hematopoietic stem/progenitor cell protein 300 (HSPC300), and Abl interactor 1 (Abi-1; Eden *et al.*, 2002). The activity of WAVE VCA domains is inhibited by intramolecular and intermolecular interactions within the WRC (Chen *et al.*, 2010). In response to upstream signals, including the activated, GTP-bound form of the Rac and Arf GTPases, acidic phospholipids, and kinases, the WRC is recruited to the membrane and undergoes conformational change to release its inhibition of WAVE (Oikawa *et al.*, 2004; Suetsugu *et al.*, 2006; Lebensohn and Kirschner, 2009; Koronakis *et al.*, 2011). WAVE1 and WAVE2 are essential in formation of dorsal and peripheral ruffles at lamellipodia during migration of embryonic fibroblasts (Suetsugu *et al.*, 2003). WAVE1, which is also known as Scar1/Wast1 (Derivery and Gautreau, 2010), is predominantly expressed in brain and plays a role in neuronal growth cone dynamics, dendritic spine morphology, and synaptic plasticity (Dahl *et al.*, 2003; Nozumi *et al.*, 2003; Soderling *et al.*, 2003, 2007; Kim *et al.*, 2006). Whether the WAVE complexes also function in endocytosis is unclear.

Previously we found that retrolinkin, a neuronal membrane protein, interacts with endophilin A1 through its proline-rich domain (PRD) and mediates endocytosis, early endocytic trafficking, and signaling of the BDNF–TrkB signal complex during dendrite outgrowth. Here we report that retrolinkin recruits the WAVE1 complex through direct interaction with CYFIP1/2 to facilitate actin-dependent endocytosis of BDNF–TrkB. These findings not only reveal the mechanistic role of retrolinkin in mediating internalization of BDNF–TrkB, but also identify WAVE1 as a novel regulator of receptor-mediated endocytosis at the neuronal plasma membrane.

RESULTS

Retrolinkin directly binds to the CYFIP2 subunit of the WAVE1 complex

To investigate the mechanistic role(s) of retrolinkin in endocytosis of the BDNF–TrkB signal complex, we performed glutathione *S*-transferase (GST) pull down of mouse brain lysates with the C-terminus of retrolinkin (RTLN-C, amino acids [aa] 489–574) fused to GST to identify its interaction partners other than endophilin A1 (Figure 1A). Three major bands in the silver-stained SDS–PAGE gel of bound proteins were identified and subjected to matrix-assisted laser desorption/ionization-time of flight (MALDI-TOF) mass spectrometry. Mass spectrometry analysis indicated that they were CYFIP2, NAP1, and WAVE1, respectively, all of which are components of the WAVE1 protein complex (Table 1 and Figure 1B). Immunoblotting analysis of bound proteins confirmed the presence of CYFIP2, NAP1, and WAVE1 but not N-WASP (Figure 1C). Coimmunoprecipitation (coIP) from mouse brain lysates verified that endogenous retrolinkin associates with the WAVE1 complex (Figure 1D). Of note, although antibodies against WAVE1, NAP1, and CYFIP2 could coimmunoprecipitate each other, only anti-CYFIP2 could coimmunoprecipitate retrolinkin (Figure 1D), suggesting that among the components of the WAVE1 complex, CYFIP2 is the direct interaction partner for retrolinkin. To determine which component of the WAVE1 complex directly interacts with retrolinkin, we performed coIP assay with lysates of transiently transfected HEK293 cells coexpressing retrolinkin and Flag-tagged WAVE1, NAP1, or Myc-tagged CYFIP2, respectively, and found that only CYFIP2 could coimmunoprecipitate with retrolinkin (Figure 1E). Conversely, GST pull down from lysates of HEK293 cells overexpressing Myc-CYFIP2 confirmed that the extreme C-terminus of retrolinkin binds to CYFIP2 (Figure 1F). To map retrolinkin interaction site(s) in CYFIP2, we performed coIP from lysates of HEK293 cells cooverexpressing retrolinkin and Myc-tagged full-length CYFIP2 or its fragments and found that its N-terminus (aa 1–624, CYFIP2-N) interacts with retrolinkin (Figure 1G). In vitro binding assay with recombinant proteins purified from *Escherichia coli* verified direct interaction between RTLN-C and CYFIP2-N (Figure 1H). Moreover, consistent with the GST pull-down data by RTLN-C, Myc-tagged CYFIP2 could not be coimmunoprecipitated by a retrolinkin fragment truncated of the C-terminus (aa 1–465, ΔC; Figure 1I), indicating that the CYFIP2-interacting site of retrolinkin does not overlap with the N-terminal endophilin A1–binding site. Further, although GST pull-down/mass spectrometry analysis did not find CYFIP1, another component of the WAVE1 complex that is highly homologous to CYFIP2 (with 87% identity, 94% similarity in amino acid sequence), in the bound proteins, it was most likely that the gel band containing CYFIP1 was omitted from the mass spectrometry analysis. We therefore determined whether it binds to retrolinkin by coIP and GST pull-down assays and found that they did interact with each other (Figure 1, J and K).

The WAVE1 complex is required for BDNF-induced dendrite outgrowth

WAVE1 acts as a downstream effector of BDNF–TrkB signaling cascade during axonal outgrowth (Namekata *et al.*, 2010). Whether it is also involved in dendrite development is unknown. The finding that the WAVE1 complex interacts with retrolinkin prompted us to investigate its role in dendrite outgrowth induced by BDNF. To determine whether the WAVE1 complex functions in dendrite outgrowth, we performed short hairpin RNA (shRNA)–mediated RNA interference (RNAi) in primary mouse hippocampal neurons (Figure 2A).

Protein name	National Center for Biotechnology Information accession number	Molecular mass (kDa)	Sequence coverage (%)	Spectral counts	Mascot score
CYFIP2	GI: 19526988	145.59	31.2	32	108
NAP1	GI: 148695316	128.78	18.62	14	98
WAVE1	GI: 13994209	61.47	13.6	6	88

TABLE 1: Proteins that associate with GST-RTLN-C.

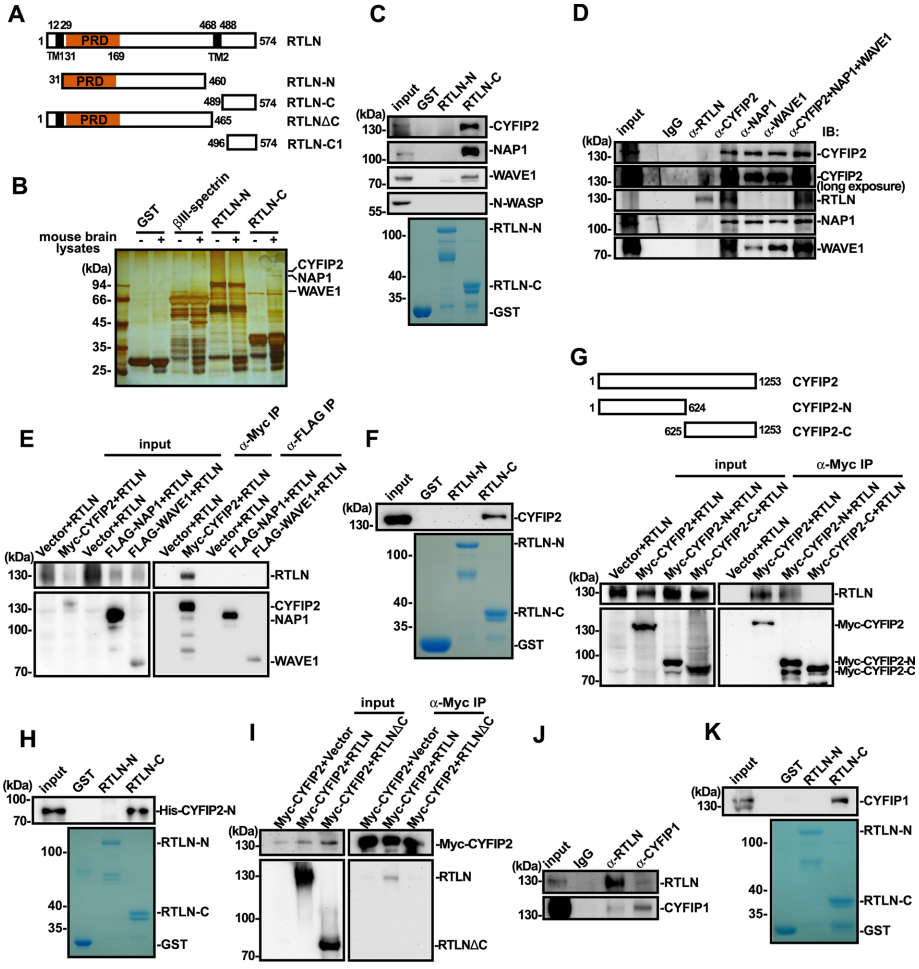

FIGURE 1: Retrolinkin interacts with the WAVE1 complex. (A) Schematic representation of the domain structure of retrolinkin (RTLN) and its fragments used in this study. PRD, proline-rich domain; TM, putative transmembrane region. (B) Lysates from adult mouse brain were subjected to GST pull down using GST-tagged RTLN-N (aa 31–460) and RTLN-C (aa 489–574). Shown is silver stained SDS–PAGE gel of bound proteins. (C) Input and bound proteins from B were analyzed by SDS–PAGE and immunoblotting with antibodies as indicated. (D) Lysates from adult mouse brain were subjected to coIP using antibodies against RTLN, CYFIP2, NAP1, WAVE1, or a combination of antibodies. Input and immunoprecipitates were analyzed by SDS–PAGE and immunoblotting with antibodies as indicated. (E) Lysates from HEK 293T cells transfected as shown at the top were subjected to coIP assay with antibodies against Myc or FLAG. Input and bound proteins were analyzed by SDS–PAGE and immunoblotting with antibodies to Myc, FLAG, and RTLN. (F) Lysates from HEK 293T cells overexpressing Myc-CYFIP2 were subjected to GST pull-down assay using GST-tagged RTLN-N and RTLN-C. (G) Lysates from HEK 293T cells expressing Myc-tagged CYFIP2 fragments (CYFIP2-N [aa 1–624] and CYFIP2-C [aa 625–1253], top) were subjected to coIP assay with antibodies against Myc. Input and immunoprecipitates were analyzed by SDS–PAGE and immunoblotting with antibodies against Myc and RTLN (bottom). (H) Recombinant His-tagged CYFIP2-N (aa 1–624) purified from *E. coli* was subjected to GST pull-down assay using GST-tagged RTLN-N and RTLN-C. GST serves as negative control. (I) Lysates from HEK 293T cells coexpressing Myc-tagged CYFIP2 and full-length or truncated RTLN (shown in A) were subjected to coIP assay with antibodies against Myc. Bound proteins were analyzed by SDS–PAGE and immunoblotting with antibodies against Myc and RTLN. (J) Lysates from adult mouse brain were subjected to coIP using antibodies against RTLN or CYFIP1. Input and immunoprecipitates were analyzed by SDS–PAGE and immunoblotting with antibodies against RTLN and CYFIP1. (K) Lysates from adult mouse brain were subjected to GST pull down using GST-tagged RTLN-N and RTLN-C. Input and bound proteins were analyzed by SDS–PAGE and immunoblotting with antibodies against CYFIP1. CBB, Coomassie brilliant blue staining.

Confocal microscopy analysis indicated that similar to retrolinkin depletion, WAVE1 depletion impaired dendrite complexity and outgrowth (Figure 2, B–E) without apparent effects on either axon length or soma size (Figure 2, F–H). Of interest, although no change in the total length of dendrites was observed in CYFIP1- or CYFIP2-depleted neurons, double knockdown of CYFIP1/2 caused dramatic decrease in dendrite length, suggesting redundancy in their function (Figure 2, B–D). Moreover, whereas knockdown of either CYFIP1 or CYFIP2 caused a reduction in the total length of dendritic branches, double knockdown caused further reduction (Figure 2E), indicating that both proteins contribute to outgrowth of dendritic branches. Of note, although N-WASP, another member of the WASP family that is also highly expressed in neuronal tissues, has been reported to play important roles in axonal outgrowth of spinal commissural neurons and dendritic spine morphogenesis of excitatory neurons (Irie and Yamaguchi, 2002; Shekarabi *et al.*, 2005), depletion of N-WASP had no effect on axonal or dendritic outgrowth of hippocampal neurons (Figure 2, B–G), suggesting that it plays distinct roles at early stages of neuronal development. Moreover, the dendrite outgrowth defect caused by WAVE1 knockdown was rescued by coexpression of an RNAi-resistant mutant of WAVE1 (Figure 2, I–M), indicating that the WAVE1-knockdown effect was specific.

Next we determined whether WAVE1 functions in BDNF-induced dendrite outgrowth. Hippocampal neurons were treated with 25 ng/ml BDNF in addition to the B27 supplement in culture medium on day in vitro 1 (DIV1), and neuronal morphology was observed on DIV5. Consistent with previous studies (Fu *et al.*, 2011), depletion of retrolinkin impaired BDNF-induced dendrite outgrowth (Figure 3, A–E). Depletion of WAVE1 but not N-WASP caused similar effects (Figure 3, A–E), indicating that it is also involved in BDNF signaling during dendritogenesis. Double but not single knockdown of CYFIP1 and CYFIP2 also impaired BDNF-induced dendrite outgrowth (Figure 3, A–E), supporting the notion that these two proteins are functionally redundant in WAVE1 complex–mediated dendrite outgrowth. Consistently, the defect in BDNF-induced dendrite outgrowth caused by WAVE1 knockdown was also rescued by coexpression of the RNAi-resistant mutant of WAVE1 (Figure 3, F–I).

The WAVE1 complex is required for BDNF–TrkB endocytosis and BDNF-induced acute ERK activation

Binding of BDNF not only activates TrkB, it also triggers internalization of the ligand–receptor complex, which is then transported in the form of signaling endosomes to mediate downstream signaling events (Kaplan and Miller, 2000; Huang and Reichardt, 2003; Segal, 2003). Although the role of WAVE1 in

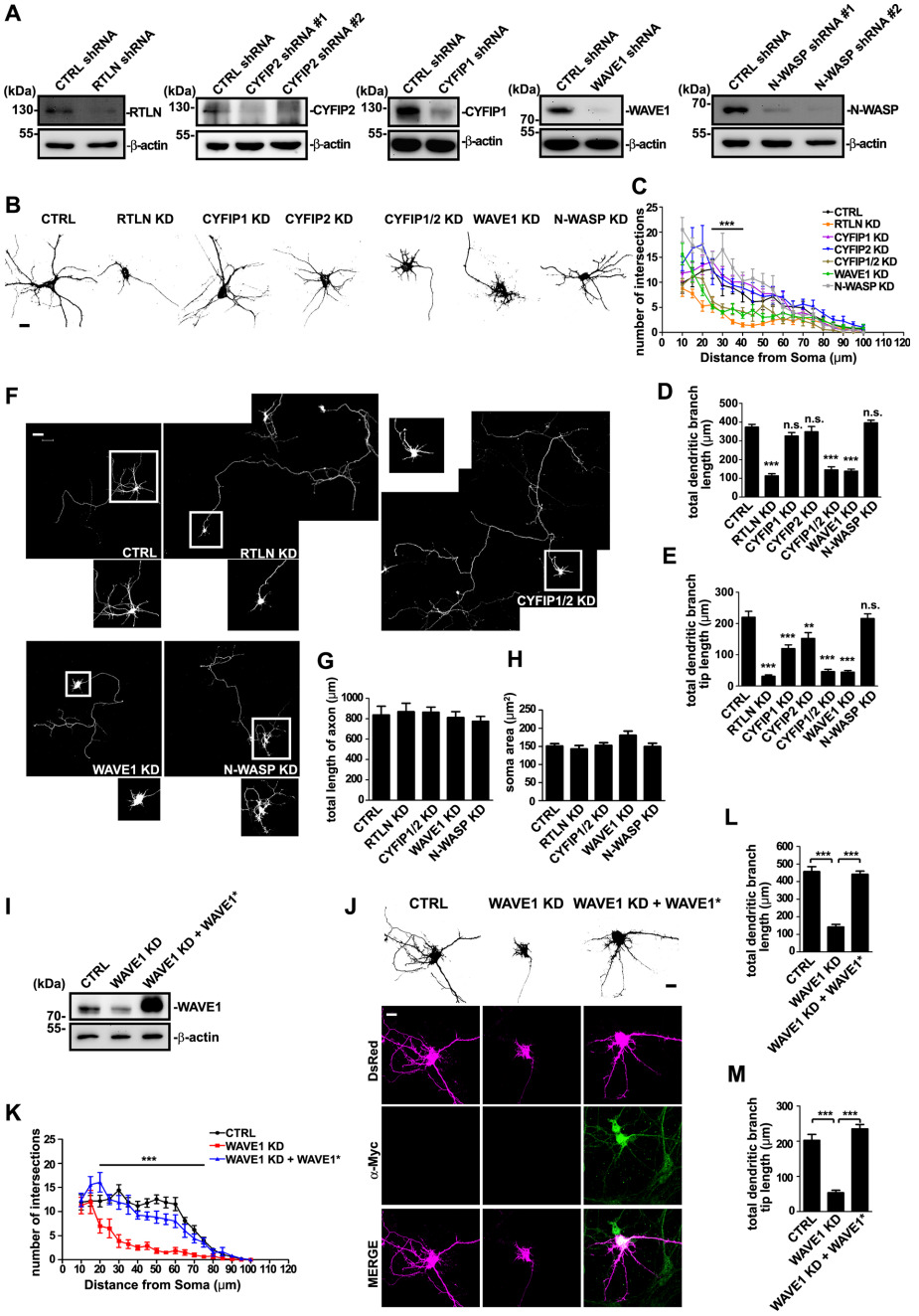

generating membrane protrusions during cell migration is well established, whether it is also involved in endocytosis is unclear. The finding that the WAVE1 complex interacts with retrolinkin prompted us to investigate its role in endocytosis of the BDNF–TrkB ligand–receptor complex. A surface biotinylation assay on lentivirus-transduced hippocampal neurons indicated that, in agreement with the results from the neuronal morphology assay, depletion of either retrolinkin or WAVE1, but not N-WASP, caused a block of BDNF-triggered TrkB endocytosis (Figure 4, A and B). Consistently, whereas knockdown of neither CYFIP1 nor CYFIP2 affected TrkB uptake, depletion of both proteins also caused a block of TrkB internalization (Figure 4, A and B). To confirm the role of WAVE1 in ligand-induced, receptor-mediated endocytosis, we overexpressed FLAG-tagged TrkB in hippocampal neurons by transient transfection and monitored its internalization with live-fed fluorescein isothiocyanate (FITC)–conjugated anti-FLAG antibodies (Fu *et al.*, 2011). Confocal microscopy revealed that, indeed, BDNF-triggered endocytosis of FLAG-TrkB was greatly impaired in WAVE1-depleted neurons (Figure 4, C and D; Supplemental Figure S1). Moreover, internalization of Alexa Fluor 488–conjugated transferrin molecules was also inhibited in WAVE1-depleted neurons (Figure 4, E and F; Supplemental Figure S1). Together these results indicate that WAVE1 is required for receptor-mediated endocytosis in CNS neurons.

Previously we showed that retrolinkin coordinates with endophilin A1 to mediate early endocytic trafficking of BDNF–TrkB and signaling from early endosomes (Fu *et al.*, 2011). To determine whether WAVE1 is involved in the retrolinkin-mediated endocytic pathway that is required for acute activation of ERK on early endosomes, we examined the phosphorylation kinetics of extracellular signal–regulated kinase (ERK)

FIGURE 2: The WAVE1 complex is required for dendritic outgrowth. (A) Mouse hippocampal neurons were infected with lentivirus expressing shRNA for 6 d. Protein levels of RTLN, CYFIP2, CYFIP1, WAVE1, or N-WASP and actin were detected by SDS–PAGE and immunoblotting of whole-cell lysates. (B) Hippocampal neurons were transfected at DIV1 with shRNA constructs coexpressing DsRed and fixed at DIV5, followed by immunostaining with antibodies against DsRed. Scrambled nontargeting shRNA served as control (CTRL). Shown are the somatodendritic regions of transfected neurons. Scale bar, 10 μm. (C) Sholl analysis was performed to quantify dendritic complexity of transfected hippocampal neurons in B; 30–40 transfected neurons per group were analyzed. All values are shown as mean ± SEM ($N = 3$). (D, E) Quantification of total dendritic branch length (D) and total dendritic branch tip length (E) from neurons in B. (F) Full view of neurons transfected and immunostained as described in B. Bottom, enlargements of boxed somatodendritic regions. Scale bar, 50 μm. (G, H) Quantification of axon length (G) and soma size (H) of transfected neurons in F. Shown are average axon length (± SEM) and soma size (± SEM) of 30–40 neurons ($N = 3$). (I) Expression constructs for control shRNA, WAVE1 shRNA, or WAVE1 shRNA and Myc-tagged RNAi-resistant WAVE1 (WAVE1*) were transfected into HEK 293T cells cultured in six-well plates. Cell lysates were analyzed by SDS–PAGE and immunoblotting with antibodies against WAVE1 and β-actin. (J) Hippocampal neurons were transfected at DIV1 with a construct coexpressing DsRed and control or WAVE1 shRNA or cotransfected with WAVE1 shRNA and WAVE1 RNAi-resistant expression construct and fixed at DIV5. RNAi-resistant WAVE1 was immunostained with anti-Myc. Scale bar, 10 μm. (K) Sholl analysis was performed on transfected hippocampal neurons in J. (L, M) Quantification of total dendritic branch length (L) and total dendritic branch tip length (M) from neurons in J. Data from 30–35 neurons. All values are shown as mean ± SEM ($N = 3$). One-way ANOVA was used to determine significance for all comparisons. $^{**}p < 0.01$, $^{***}p < 0.001$, n.s., not significant.

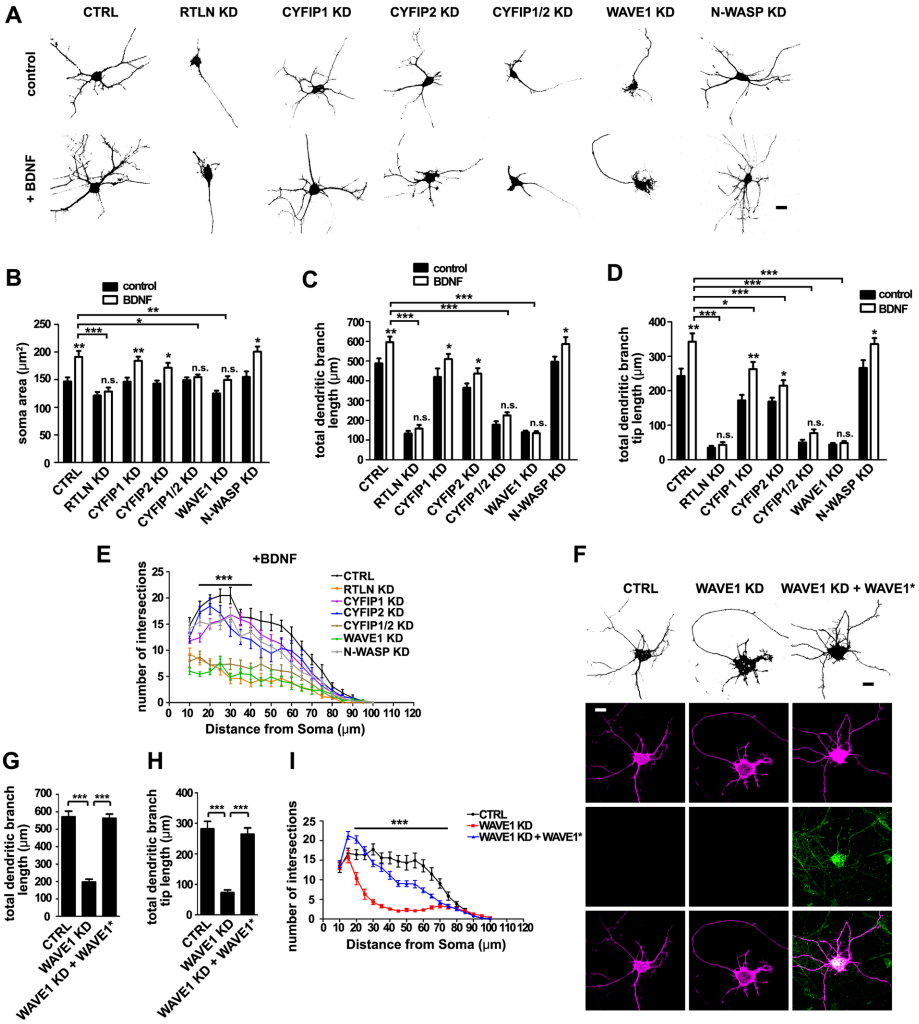

FIGURE 3: The WAVE1 complex is required for BDNF-induced dendritic outgrowth. (A) Hippocampal neurons were transfected at DIV1 with shRNA constructs coexpressing DsRed, cultured for 4 d in the presence of BDNF (25 ng/ml) after transfection, fixed at DIV5, and immunostained with antibodies against DsRed. Scale bar, 10 μm. (B–E) Quantification of soma area (B), total dendritic branch length (C), total dendritic branch tip length (D), and Sholl analysis (E) from neurons in A; 20–30 transfected neurons were analyzed. All values are shown as mean ± SEM ($N = 2$). Note that data for control groups are omitted from E for better visualization. (F) Hippocampal neurons were transfected at DIV1 with constructs coexpressing DsRed and shRNA or cotransfected with WAVE1 shRNA and WAVE1 RNAi-resistant (WAVE1*) expression constructs. Cells were then cultured for 4 d in the presence of BDNF (25 ng/ml) after transfection, fixed at DIV5, and immunostained with antibodies against anti-Myc. Scale bar, 10 μm. (G–I) Quantification of total dendritic branch length (G), total dendritic branch tip length (H), and Sholl analysis (I) from neurons in F. Data from 30–35 neurons. All values are shown as mean ± SEM ($N = 3$). *$p < 0.05$, **$p < 0.01$, ***$p < 0.001$. n.s., not significant.

and Akt in BDNF-stimulated neurons. Indeed, immunoblotting analysis revealed that, similar to retrolinkin knockdown, shRNA-mediated knockdown of WAVE1 impaired acute activation of ERK in neurons treated with BDNF, whereas neither prolonged activation of ERK nor the kinetics of Akt activation was affected (Figure 4, G and H). In contrast, depletion of N-WASP did not affect BDNF–TrkB endocytosis and signaling (Figure 4, A–D, G, and H). Nevertheless, in good agreement with previous findings (Kessels and Qualmann, 2002; Innocenti *et al.*, 2005), N-WASP knockdown impaired receptor-mediated endocytosis of transferrin in hippocampal neurons (Figure 4, E and F). Together these results indicate that both retrolinkin and WAVE1 are required for BNDF-induced acute ERK activation via endocytic trafficking of activated TrkB.

Accumulation of WAVE1 at the endocytic sites of BDNF-activated TrkB requires retrolinkin

Internalization of neurotrophin-activated Trk receptors occurs via both clathrin-dependent and pincher-dependent pathways (Beattie *et al.*, 2000; Valdez *et al.*, 2005). Actin polymerization plays an essential role in clathrin-mediated endocytosis, which is required for invagination and scission of cargo-loaded clathrin-coated vesicles (CCV) from plasma membrane (Merrifield *et al.*, 2005). Whether and how the NPFs are recruited to endocytic sites of BDNF-activated TrkB to promote actin polymerization remains unknown. Although data from aforementioned knockdown experiments showed that WAVE1 is required for endocytosis of BDNF-activated TrkB, coIP assay using antibodies against WAVE1 or Trk receptors did not detect interaction between WAVE1 and Trk (Figure 5A). In addition, although studies reveal a highly conserved peptide motif shared by potential WRC ligands that binds to an interaction surface formed by the Sra/CYFIP and Abi components of the WRC (Chen *et al.*, 2014), we did not identify similar sequence motif(s) in either retrolinkin or TrkB. Having found that retrolinkin interacts with the CYFIP1/2 subunit of the WAVE1 complex and that WAVE1 is required for endocytosis and signaling of BDNF-activated TrkB, we reasoned that retrolinkin might function by recruiting the WAVE1 complex to endocytic sites of activated TrkB to promote actin polymerization. To determine whether retrolinkin regulates TrkB endocytosis through its interaction with WAVE1, first we examined the colocalization of WAVE1 with activated TrkB (pTrk) upon BDNF stimulation. Quantitative analysis of confocal images showed that, whereas the mean fluorescence intensity of pTrk signals in neurons increased upon BDNF addition and kept increasing during the time monitored (Figure 5B), in agreement with the dynamics of both clathrin-dependent and -independent endocytosis (Merrifield *et al.*, 2005; Mettlen *et al.*, 2009; Basquin *et al.*, 2015), colocalization between WAVE1 and ligand-activated TrkB (pTrk) in hippocampal neurons increased and peaked at 2 min after BDNF addition, indicating that WAVE1 was recruited to the sites of BDNF–TrkB endocytosis or clathrin-coated pits containing activated TrkB (Figure 5, C and D; see Supplemental Figure S2 for testing of antibodies to pTrk for immunofluorescence staining). Indeed, although no change in expression levels of WAVE1 was detected in retrolinkin-depleted neurons (Figure 5E), there was a significant decrease in colocalization between WAVE1 and pTrk at the 2-min time point after BDNF addition in retrolinkin-depleted neurons (Figure 5, F and G), indicating that accumulation of WAVE1 at the sites of pTrk endocytosis requires retrolinkin.

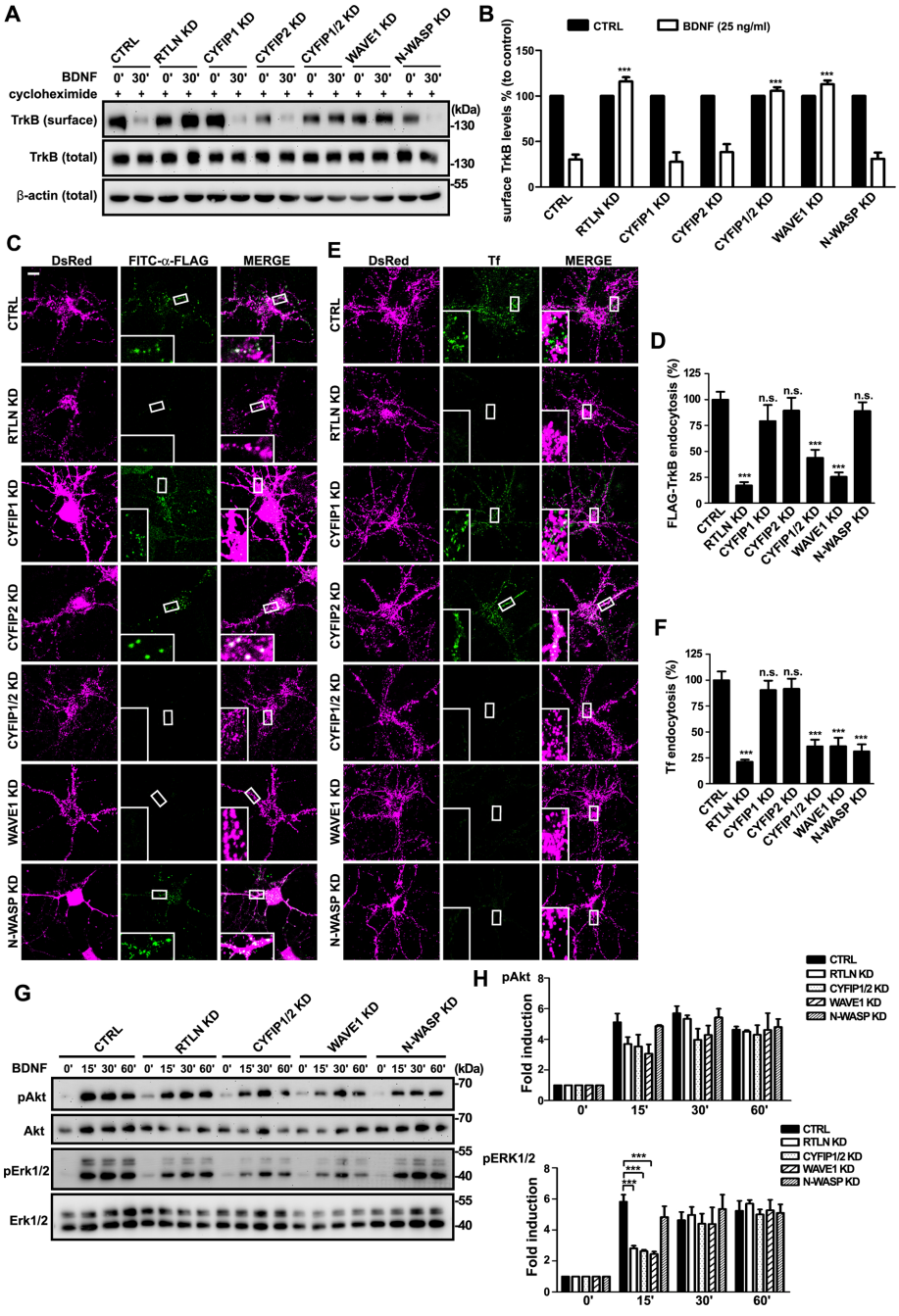

FIGURE 4: The WAVE1 complex, not N-WASP, is required for BDNF-induced endocytosis of TrkB and acute Erk activation. (A) Cortical neurons infected with shRNA-expressing lentivirus were treated with BDNF (25 ng/ml) for 30 min. Endocytosis of TrkB was then measured by cleavable surface biotinylation. Surface TrkB was detected by immunoblotting of biotinylated proteins with anti–pan-Trk. Total TrkB and β-actin were detected by immunoblotting of whole-cell lysates. (B) Quantification of immunoblotting results in A. Values were normalized to the respective TrkB levels of control. All values are shown as mean ± SEM ($N = 3$). (C) Hippocampal neurons were cotransfected with FLAG-TrkB and shRNA-expressing constructs at DIV4. Neurons were treated with BDNF (25 ng/ml) for 30 min at DIV8. Internalized FLAG-TrkB was labeled with FITC–α-FLAG. Insets, enlarged images of the boxed regions. (D) Quantification of TrkB endocytosis in neurons in C by measuring mean fluorescence intensity of FLAG-TrkB puncta per neuron (35 neurons from three independent experiments). (E) Hippocampal neurons were transfected with shRNA constructs at DIV4 and treated with 10 μg/ml Alexa Fluor 488–conjugated transferrin (Tf) for 15 min at DIV8. Insets, enlarged images of the boxed regions. (F) Quantification of Tf uptake in neurons in E by measuring mean fluorescence intensity of Tf puncta per cell (42 neurons from three independent experiments). (G) Cortical neurons infected with shRNA-expressing lentivirus were treated with BDNF for different periods. Levels of the total and phosphorylated proteins were detected by SDS–PAGE and immunoblotting. (H) Quantitative analysis of the immunoblot bands in G. Average pAkt and pERK1/2 levels were normalized to levels detected at the 0-min time point and represented as fold induction. Data represent mean ± SEM ($N = 3$). ***$p < 0.001$, n.s., not significant. Scale bar, 10 μm.

Disruption of retrolinkin-CYFIP1/2 interaction impairs recruitment of WAVE1 to the plasma membrane, BDNF-TrkB endocytosis, and signaling

Given that retrolinkin interacts with the CYFIP1/2 subunits of the WAVE regulatory complex and that the colocalization between WAVE1 and BDNF-activated TrkB during endocytosis requires retrolinkin, we reasoned that retrolinkin recruits WAVE1 through its interaction with CYFIP1/2 to the plasma membrane to facilitate BDNF–TrkB endocytosis and signaling. To determine whether the interaction between retrolinkin and CYFIP1/2 is required for the recruitment of the WAVE1 complex to the sites of TrkB endocytosis, first we tested whether a retrolinkin mutant truncated of the C-terminal CYFIP1/2-interaction domain (RTLNΔC) would rescue dendrite outgrowth phenotype of retrolinkin-depleted neurons (Figure 1, A and I). Overexpression of the RNAi-resistant RTLNΔC did not rescue the dendrite complexity and outgrowth phenotype of retrolinkin-depleted neurons (Figure 6, A–D), indicating that the CYFIP1/2-interacting C-terminus of retrolinkin is required for its function in dendrite development. Consistently, overexpression of the RTLNΔC mutant also failed to rescue impairment in BDNF-induced dendrite outgrowth caused by retrolinkin knockdown (Figure 6, E–H).

Next we overexpressed the C-terminus of retrolinkin in neurons (Figures 1A and 7A). We reasoned that binding of a cytosolic retrolinkin fragment to CYFIP1/2 would sequester these molecules and prevent them from interacting with the endogenous full-length retrolinkin. By doing so, retrolinkin would not be able to recruit the WAVE1 complex to BDNF–TrkB endocytic sites, so that internalization of the ligand–receptor complex would be blocked. Indeed, overexpression of a retrolinkin C-terminal fragment that binds to CYFIP2 (RTLN–C1) (Figures 1A and 7A) caused a significant decrease in colocalization between WAVE1 and pTrk upon BDNF stimulation (Figure 7, B and C), indicating that it impaired recruitment of WAVE1 to BDNF–TrkB endocytic sites. Consistently, in neurons overexpressing RTLN–C1, not only was endocytosis of BDNF-activated TrkB impaired (Figure 7, D and E, and Supplemental Figure S3), but also dendrite

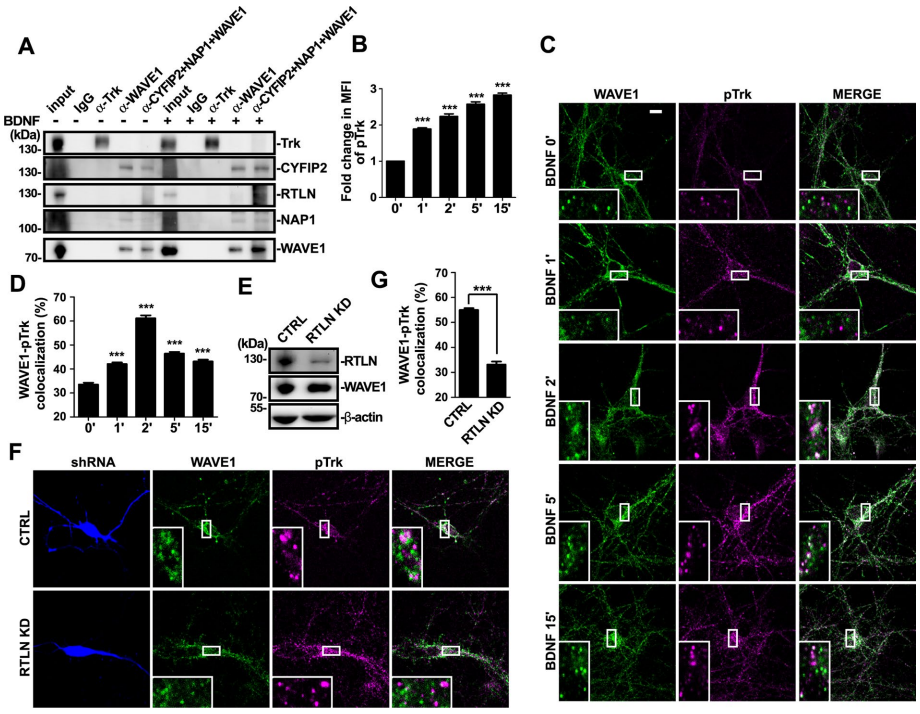

FIGURE 5: Retrolinkin is required for recruitment of WAVE1 to TrkB endocytic sites. (A) Cultured cortical neurons with or without BDNF stimulation were subjected to coIP using antibodies against pan-Trk, WAVE1, or a combination of antibodies to CYFIP2, NAP1, and WAVE1. Bound proteins were analyzed by SDS–PAGE and immunoblotting with antibodies against pan-Trk, CYFIP2, RTLN, NAP1, and WAVE1. (B) DIV7 hippocampal neurons expressing DsRed were starved for 2 h, stimulated with BDNF (25 ng/ml) for different periods, and immunostained with antibodies against phosphorylated Trk (pTrk), the activated form of Trk. Quantification of changes in mean fluorescence intensity (MFI) of pTrk signal over time; 30 neurons. (C) DIV7 hippocampal neurons were starved for 2 h, stimulated with BDNF (25 ng/ml) for different periods, and double stained with antibodies against WAVE1 and pTrk. (D) Quantification of the colocalization between WAVE1 and pTrk. Thirty neurons from three independent experiments were analyzed. (E) Hippocampal neurons infected with RTLN shRNA–expressing lentivirus were lysed and analyzed by immunoblotting with antibodies to RTLN and WAVE1. (F) Hippocampal neurons transfected with shRNA-expressing constructs were starved for 2 h, stimulated with BDNF for 2 min, and double stained with antibodies against WAVE1 and pTrk. (G) Quantification of the colocalization between WAVE1 and pTrk in transfected neurons in F. Thirty neurons from three independent experiments were analyzed. Data represent mean ± SEM ($N = 3$). ***$p < 0.001$. Scale bar, 10 μm.

outgrowth with or without BDNF was affected compared with that in control neurons (Figure 7, F–M). Together these data indicate that the interaction between retrolinkin and CYFIP1/2 is required for recruitment of WAVE1 to the plasma membrane to promote BDNF–TrkB endocytosis and signaling during dendrite outgrowth.

The WAVE1 complex accelerates actin polymerization through Arp2/3 at the endocytic site of the BDNF–TrkB signal complex

Because retrolinkin recruits WAVE1 to endocytic sites of BDNF-activated TrkB, endocytosis of the ligand–receptor signal complex might be facilitated by WAVE1-promoted actin polymerization. To determine whether endocytosis of BDNF-TrkB requires actin polymerization, we examined the effect of latrunculin A, a sponge toxin that binds and sequesters actin monomers (G-actin) from polymerizing (Coue *et al.*, 1987; Spector *et al.*, 1989), on internalization of Flag-TrkB in hippocampal neurons upon BDNF stimulation. Indeed, latrunculin A treatment caused not only a decrease in the content of polymerized actin (F-actin) as detected by the fluorescence intensity of phalloidin—a mushroom toxin that selectively binds and labels F-actin (Wulf *et al.*, 1979; Figure 8A)—but also a significant decrease in the amount of endocytosed fluorescence-labeled Flag-TrkB (Figure 8, B and C, and Supplemental Figure S4), indicating that the ligand-induced endocytosis of TrkB is actin polymerization dependent.

Next we asked whether WAVE1 is required for actin polymerization at the sites of BDNF–TrkB endocytosis. To determine whether silencing of WAVE1 affects actin polymerization that is required for TrkB endocytosis, we transfected neurons with a WAVE1 shRNA–expressing construct and monitored colocalization between activated TrkB (pTrk) and phalloidin-labeled F-actin upon BDNF treatment. Confocal microscopy analysis indicated that, compared with control cells, there was a significant decrease in colocalization between pTrk and phalloidin puncta in WAVE1-depleted neurons (Figure 8D), indicating that WAVE1 activity is required for actin polymerization during endocytosis of BDNF-activated TrkB endocytosis.

Because WAVE1 stimulates the nucleation activity of the Arp2/3 complex to accelerate branched actin polymerization, we attempted to test whether Arp2/3 is recruited to the endocytic sites of BDNF-TrkB upon BDNF addition. Unfortunately, immunostaining with antibodies against the p34 or the Arp2 subunit of Arp2/3 gave rise to strong diffuse fluorescence signals with no particular pattern throughout the neuronal cytoplasm, preventing us from assessing colocalization between Arp2/3 and endocytosed TrkB puncta by quantitative analysis, given the high background of Arp2/3 immunofluorescence signals. As an alternative approach to determine whether Arp2/3 plays a role in BDNF-induced TrkB internalization, an inhibitor of Arp2/3 activity, CK-666 (Nolen *et al.*, 2009), was applied to hippocampal neurons. Immunostaining and confocal microscopy analysis revealed that, indeed, CK-666 treatment caused not only a decrease in F-actin content (Figure 8E) but also a huge reduction in the amount of endocytosed Flag-TrkB (Figure 8, F and G, and Supplemental Figure S4), whereas it had no effect on colocalization of WAVE1 with pTrk (Figure 8, H and I). Further, overexpression of the C-terminal fragment of human WAVE1 (Scar-WA) in neurons, which binds to the p21 subunit of the Arp2/3 complex and serves as dominant-negative mutant to disrupt its localization (Machesky and Insall, 1998), also severely impaired internalization of TrkB upon BDNF stimulation and accumulation of F-actin at sites of TrkB activation (Figure 8, J–L, and Supplemental Figure S4). Together these results indicate that Arp2/3 is required for endocytosis of BDNF-activated TrkB and works downstream of the WAVE1 complex.

Next, to verify that retrolinkin recruits WAVE1 through CYFIP1/2 to promote actin polymerization at BDNF-TrkB endocytic sites, we overexpressed the retrolinkin C-terminus as dominant-negative mutant to disrupt the interaction between full-length retrolinkin and

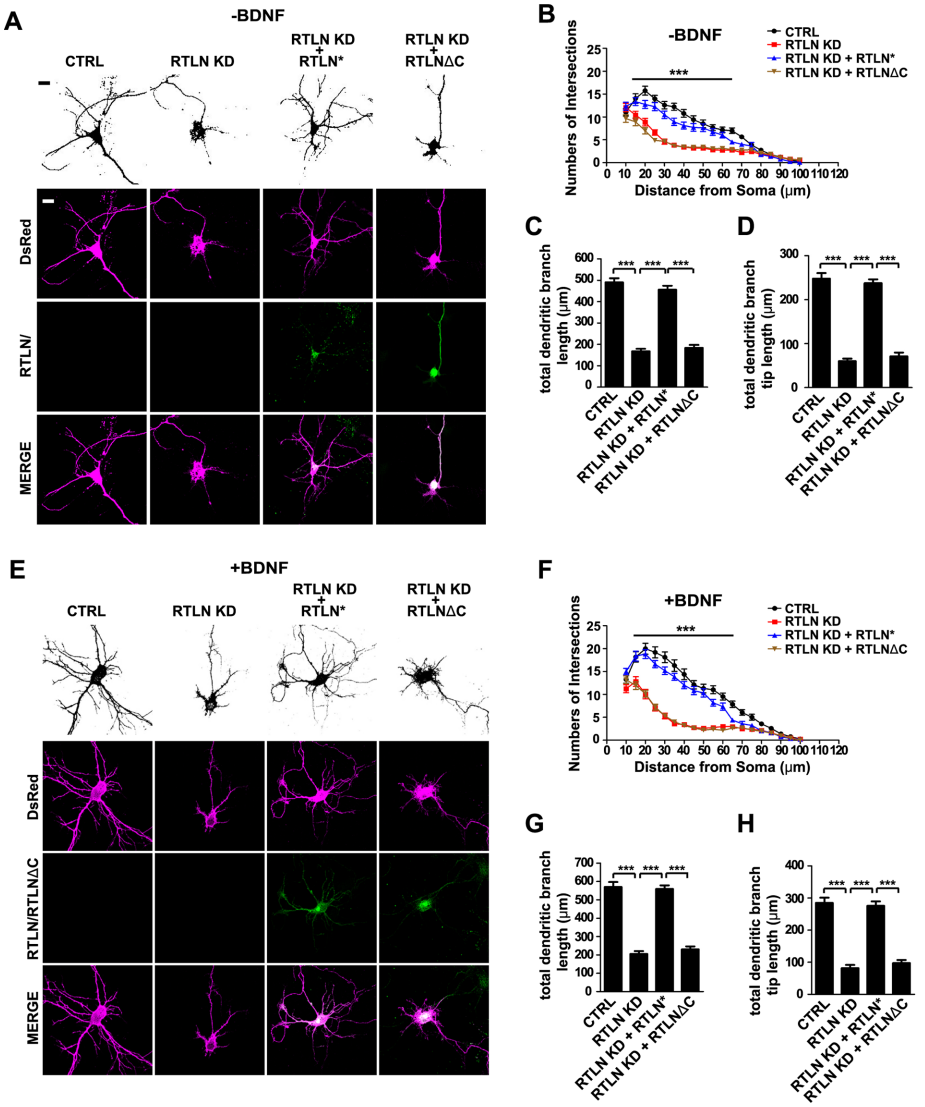

FIGURE 6: The C-terminal CYFIP-binding region of retrolinkin is required for dendritic outgrowth. (A) Hippocampal neurons were transfected at DIV1 with shRNA constructs coexpressing DsRed or cotransfected with shRNA and RNAi-resistant (RTLN*) RTLN or RTLNΔC expression constructs (shown in Figure 1A) and fixed at DIV5, followed by immunostaining with antibodies against DsRed and RTLN. Scale bar, 10 μm. (B–D) Sholl analysis (B), quantification of total dendritic branch length (C), and total dendritic branch tip length (D) from neurons in A. Data from 30–35 neurons. All values are shown as mean ± SEM ($N = 3$). (E) Hippocampal neurons were transfected as described in A and cultured for 4 d in the presence of BDNF (25 ng/ml) after transfection. (F–H) Sholl analysis (F), quantification of total dendritic branch length (G), and total dendritic branch tip length (H) from neurons in E. Data from 30–35 neurons. All values are shown as mean ± SEM ($N = 3$). ***$p < 0.001$. Scale bar, 10 μm.

CYFIP1/2 in neurons and monitored accumulation of F-actin around BDNF-activated TrkB/pTrk. Overexpression of RTLN-C1 caused a significant decrease in colocalization between pTrk and phalloidin puncta (Figure 8M), indicating that the interaction between retrolinkin and CYFIP1/2 is required for actin polymerization during BDNF–TrkB endocytosis.

WAVE1-mediated, actin-dependent endocytosis of BDNF–TrkB is clathrin independent

Finally, to determine whether WAVE1-mediated, actin-dependent endocytosis of activated TrkB is clathrin dependent or not, we treated neurons cotransfected with Flag-TrkB and DsRed expression constructs with the CME inhibitors chlorpromazine and Pitstop2 (Wang *et al.*, 1993; von Kleist *et al.*, 2011). Unfortunately, both drugs were so toxic to neurons that we did not detect fluorescence signals of Flag-TrkB on the plasma membrane of drug-treated transfected cells (Supplemental Figure S5). As an alternative approach, we overexpressed the DIII mutant of the AP-2–interacting protein Eps15, which interferes with the assembly of clathrin-coated pits (CCPs; Benmerah *et al.*, 1998, 1999, 2000), in hippocampal neurons. Consistent with previous findings (Benmerah *et al.*, 1998), transferrin uptake was largely inhibited in neurons overexpressing Eps15 DIII but not those overexpressing enhanced GFP (EGFP) or Eps15 DIIIΔ2, another Eps15 mutant that is deleted of AP-2–binding sites and does not inhibit CCP assembly (Figure 9, A and B). In contrast, overexpression of Eps15 DIII caused only ~30% decrease in BDNF-induced endocytosis of TrkB (Figure 9, C and D). Moreover, confocal microscopy and colocalization analysis showed that neither the colocalization between pTrk and WAVE1 nor that between pTrk and phalloidin was affected in neurons expressing Eps15 DIII (Figure 9, E–G). Together these data suggest that WAVE1-mediated actin-dependent endocytosis of BDNF-activated TrkB in the somatodendritic region of hippocampal neurons is clathrin independent.

DISCUSSION

In this study, we present evidence that retrolinkin mediates BDNF-induced endocytosis of TrkB by recruiting the WAVE1 protein complex to the plasma membrane to promote actin polymerization (Supplemental Figure S6). Retrolinkin directly binds to the CYFIP1/2 subunits of the WAVE1 complex through its C-terminus. Both retrolinkin and WAVE1 are required for BDNF–TrkB endocytic trafficking and signaling, whereas N-WASP, another member of the WASP family that has been shown to function in endocytosis in fibroblasts (COS7 and Swiss 3T3) and epithelial (HeLa) cells, is not required for BDNF–TrkB endocytosis and downstream signaling. By shRNA-mediated knockdown experiments we show that CYFIP1 and CYFIP2 are functionally redundant in receptor-mediated endocytosis. Disruption of the protein–protein interaction between retrolinkin and CYFIP1/2 impairs BDNF-TrkB endocytosis and BDNF-induced dendrite outgrowth. In the absence of retrolinkin, WAVE1 cannot be recruited to BDNF–TrkB endocytic sites to promote actin polymerization. Previous studies implicated Numb, an endocytic adaptor protein, and GSK3β, a kinase that phosphorylates the dynamin 1 component of the clathrin-dependent endocytic machinery, as positive and negative regulators of BDNF-dependent TrkB endocytosis, respectively (Zhou *et al.*, 2011; Liu *et al.*, 2015). Our study identifies

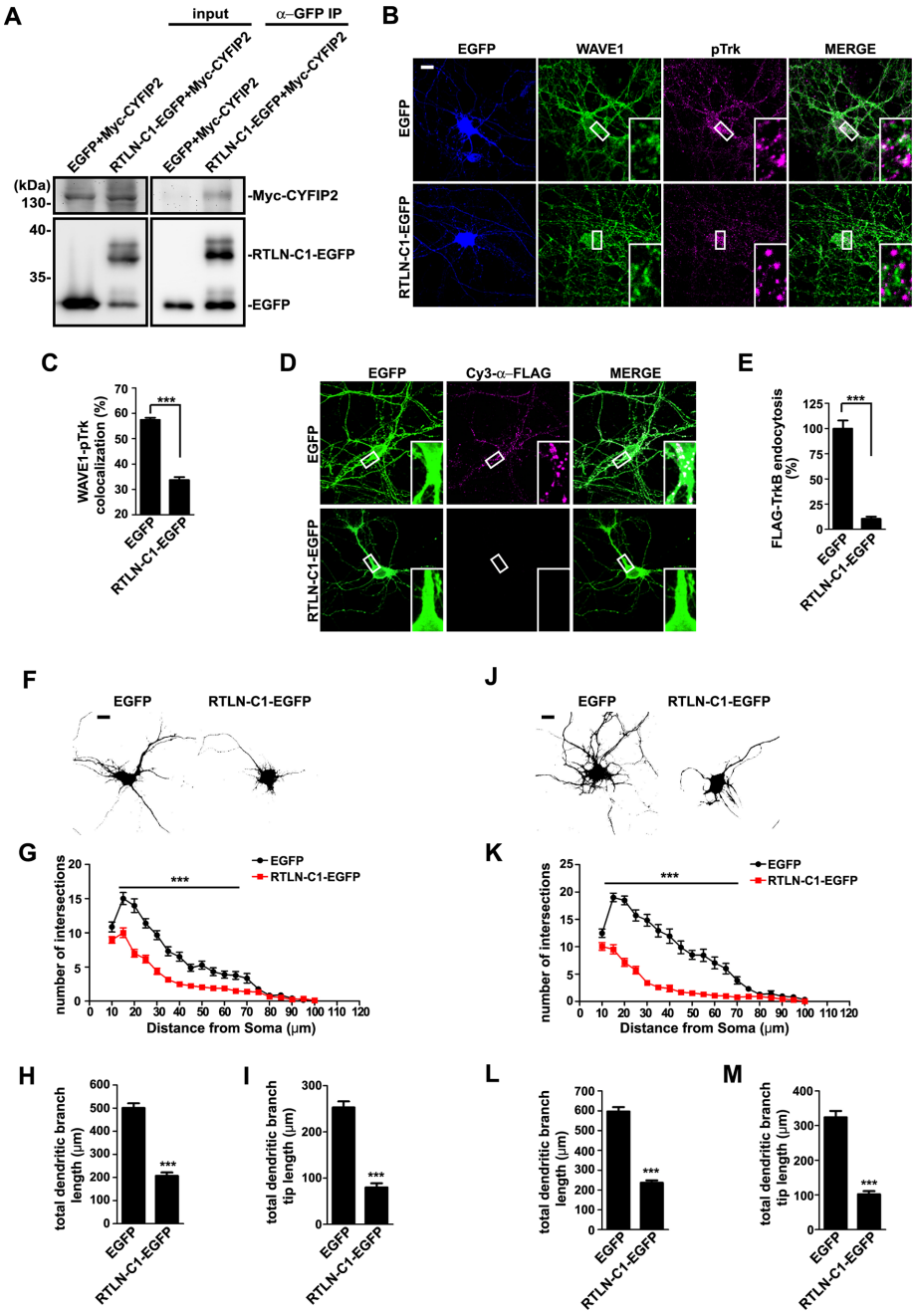

FIGURE 7: Disruption of the interaction between retrolinkin and CYFIP1/2 impairs BDNF-induced TrkB endocytosis and dendritic outgrowth. (A) Lysates from HEK 293T cells coexpressing Myc-tagged CYFIP2 and RTLN-C1-EGFP (shown in Figure 1A) were subjected to coIP assay with antibodies against GFP. Bound proteins were analyzed by SDS–PAGE and immunoblotting with antibodies against Myc and GFP. (B) Hippocampal neurons transfected with construct expressing EGFP or RTLN-C1-EGFP were starved for 2 h, stimulated with BDNF for 2 min, and immunostained with antibodies against WAVE1 and pTrk. (C) Quantification of the colocalization between WAVE1 and pTrk in B. Thirty neurons from three independent experiments were analyzed. Data represent mean ± SEM ($N = 3$). (D) Hippocampal neurons cotransfected with expression constructs for FLAG-TrkB and EGFP or RTLN-C1-EGFP were treated with BDNF (25 ng/ml) for 30 min. Internalized FLAG-TrkB was labeled with Cy3–α-FLAG. (E) Quantification of TrkB endocytosis in neurons in D by measuring mean fluorescence intensity of FLAG-TrkB puncta per neuron (35 neurons from three independent experiments). (F) Hippocampal neurons were transfected at DIV1 with EGFP or RTLN-C1-EGFP expression construct and fixed at DIV5, followed by immunostaining with anti-GFP. Scale bar, 10 μm. (G–I) Sholl analysis (G), quantification of total dendritic branch length (H), and total dendritic branch tip length (I) from neurons in F. Data from 30–35 neurons. All values are shown as mean ± SEM ($N = 3$). (J) Hippocampal neurons were transfected as described in F and cultured for 4 d in the presence of BDNF (25 ng/ml) after transfection. (K–M) Sholl analysis (K), quantification of total dendritic branch length (L), and total dendritic branch tip length (M) from neurons in J. Data from 30–35 neurons. All values are shown as mean ± SEM ($N = 3$). ***$p < 0.001$. Scale bar, 10 μm.

WAVE1 as the NPF required for endocytosis of the BDNF–TrkB signal complex in CNS neurons by promoting Arp2/3-mediated actin polymerization.

In our previous study on retrolinkin, it was predicted by a protein analysis algorithm that this protein contains two transmembrane regions, leading us to believe that both its extreme N- and C-termini are on the luminal side, with the segment of aa 30–467 exposed to the cytosol and interacting with other proteins (Liu *et al.*, 2007). However, our follow-up studies show that retrolinkin interacts with CYFIP1/2 through its extreme C-terminus (Figures 1F and 7A). Because CYFIP1/2 is a cytosolic protein, current evidence indicates that retrolinkin is a type I transmembrane protein.

In BDNF-induced TrkB endocytic trafficking and signaling, retrolinkin mediates not only endocytosis of the signal complex but also postendocytic trafficking of the signaling endosomes carrying activated TrkB via its interaction with endophilin A1 (Fu *et al.*, 2011). Nevertheless, how retrolinkin is activated upon BDNF–TrkB binding to interact with CYFIP1/2 and recruits the WAVE1 complex (Figure 5A) remains to be explored. Changes in the conformational state of retrolinkin might enhance its interaction with CYFIP1/2; another possible mechanism is via changes in its phosphorylation state, as protein sequence analysis (www.phosphosite.org/homeAction.action) predicts putative phosphorylation sites in retrolinkin. Whether and how posttranslational modification(s) of retrolinkin regulates its function in BDNF-TrkB endocytosis await further investigation.

The WASP and WAVE family proteins promote F-actin assembly by stimulating Arp2/3-dependent nucleation of actin filaments. Through interactions mediated by sites located outside of the VCA domain and the WRC, they are targeted by a variety of regulatory factors to different subcellular locations and signaling pathways to serve distinct cellular and physiological roles, for example, in endocytosis, membrane traffic, cell motility, and neuronal morphogenesis. The growth factor EGF induces recruitment of N-WASP to lipid rafts in plasma membrane and its association with endophilin

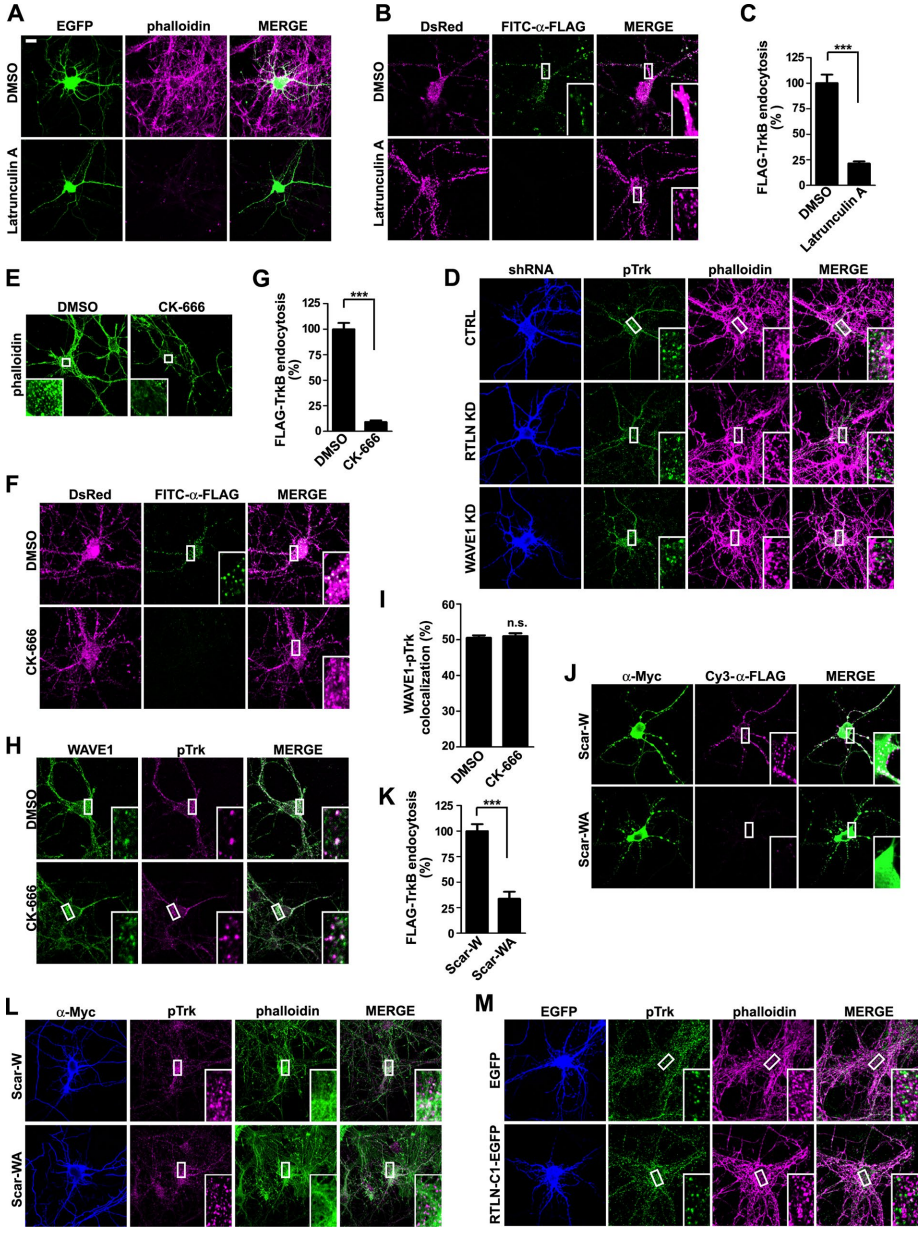

FIGURE 8: Retrolinkin regulates BDNF-TrkB endocytosis through WAVE1-activated actin polymerization. (A) Hippocampal neurons treated with DMSO (vehicle control) or latrunculin A (1 μM) for 1 h were stained with Alexa Fluor 568–conjugated phalloidin to monitor F-actin content. EGFP serves as volume marker. (B) Hippocampal neurons cotransfected with DsRed and FLAG-TrkB–expressing constructs were treated with DMSO or latrunculin A (1 μM) for 1 h, rinsed with MEM, and stimulated with BDNF (25 ng/ml) for 30 min. Internalized FLAG-TrkB was labeled with FITC–α-FLAG and analyzed by confocal microscopy. (C) Quantification of TrkB endocytosis in neurons in B by measuring mean fluorescence intensity of FLAG-TrkB puncta per cell (35 neurons from two independent experiments). (D) Hippocampal neurons transfected with construct expressing shRNA were starved for 2 h, stimulated with BDNF for 2 min, fixed, and stained with anti-pTrk and Alexa Fluor 568–conjugated phalloidin. Representative confocal images. (E) Hippocampal neurons treated with DMSO or CK-666 (200 μM) for 2 h were stained with Alexa Fluor 488–conjugated phalloidin to monitor F-actin content. (F) Hippocampal neurons cotransfected with DsRed and FLAG-TrkB–expressing constructs were treated with DMSO or CK-666 (200 μM) for 2 h, rinsed with MEM, and stimulated with BDNF (25 ng/ml) for 30 min. Internalized FLAG-TrkB was labeled with FITC–α-FLAG and analyzed by confocal microscopy. (G) Quantification of TrkB endocytosis in neurons in F by measuring mean fluorescence intensity of FLAG-TrkB puncta per cell (42 neurons from three independent experiments). (H) Hippocampal neurons were treated with DMSO or CK-666 (200 μM) for 2 h, rinsed with MEM, and stimulated with BDNF (25 ng/ml) for 2 min and immunostained with antibodies against WAVE1 and pTrk. (I) Quantification of the colocalization between WAVE1 and pTrk in H. Thirty neurons from two independent experiments were analyzed. (J) Hippocampal neurons were cotransfected with expression constructs for FLAG-TrkB and Myc-tagged Scar-W or Scar-WA at DIV4 and treated with BDNF (25 ng/ml) for 30 min at DIV8. Internalized FLAG-TrkB was labeled with Cy3-α-FLAG. Scar-W and Scar-WA were stained with anti-Myc antibody. Scar-W does not bind to Arp2/3 and serves as negative control for Scar-WA. (K) Quantification of Flag-TrkB endocytosis in neurons in J by measuring mean fluorescence intensity of FLAG-TrkB puncta per neuron (25 neurons from two independent experiments). (L) Hippocampal neurons transfected with construct expressing Myc-tagged Scar-W or Scar-WA were starved for 2 h, stimulated with BDNF for 2 min, fixed, and stained with anti-pTrk and Alexa Fluor 568–conjugated phalloidin. Representative confocal images. (M) Hippocampal neurons transfected with construct expressing EGFP or RTLN-C1-EGFP were starved for 2 h, stimulated with BDNF for 2 min, fixed, and stained with anti-pTrk and Alexa Fluor 568–conjugated phalloidin. Representative confocal images. Data represent mean ± SEM. ***$p < 0.001$, n.s., not significant. Scale bar, 10 μm.

A3, a component of the endocytic machinery and binding partner for dynamin, implicating it in clathrin-mediated endocytosis (Otsuki *et al.*, 2003). Moreover, time-lapse fluorescence microscopy imaging of fibroblast cells reveals that both N-WASP and Arp2/3, but not WAVE2, the ubiquitously expressed WAVE family member, are recruited to clathrin-coated pits (Merrifield *et al.*, 2004; Benesch *et al.*, 2005) and that N-WASP deficiency causes a reduction in the accumulation of both actin and Arp2/3 at clathrin-coated structures and a decrease in EGF internalization (Benesch *et al.*, 2005). Nevertheless, our study demonstrates that WAVE1, not N-WASP, interacts with retrolinkin and is required for receptor-mediated endocytosis of BDNF–TrkB in CNS neurons, indicating that WAVE1 and N-WASP play distinct roles in neuronal cells, as well as in other cell types. Of note, depletion of either WAVE1 or N-WASP impairs transferrin uptake at the neuronal plasma membrane, implying variance in cargo selectivity of receptor-mediated endocytosis by the actin-dependent endocytic machinery.

Actin is essential for many types of endocytosis, including phagocytosis, macropinocytosis, and the circular dorsal ruffle pathway (Mooren *et al.*, 2012). Although a role for actin polymerization in CME in yeast has been firmly established, studies in metazoan cells yielded conflicting results, indicating that the relative importance of actin in CME varies depending on cell type and experimental setting (Mooren *et al.*, 2012). Moreover, a study reported that actin depolymerization

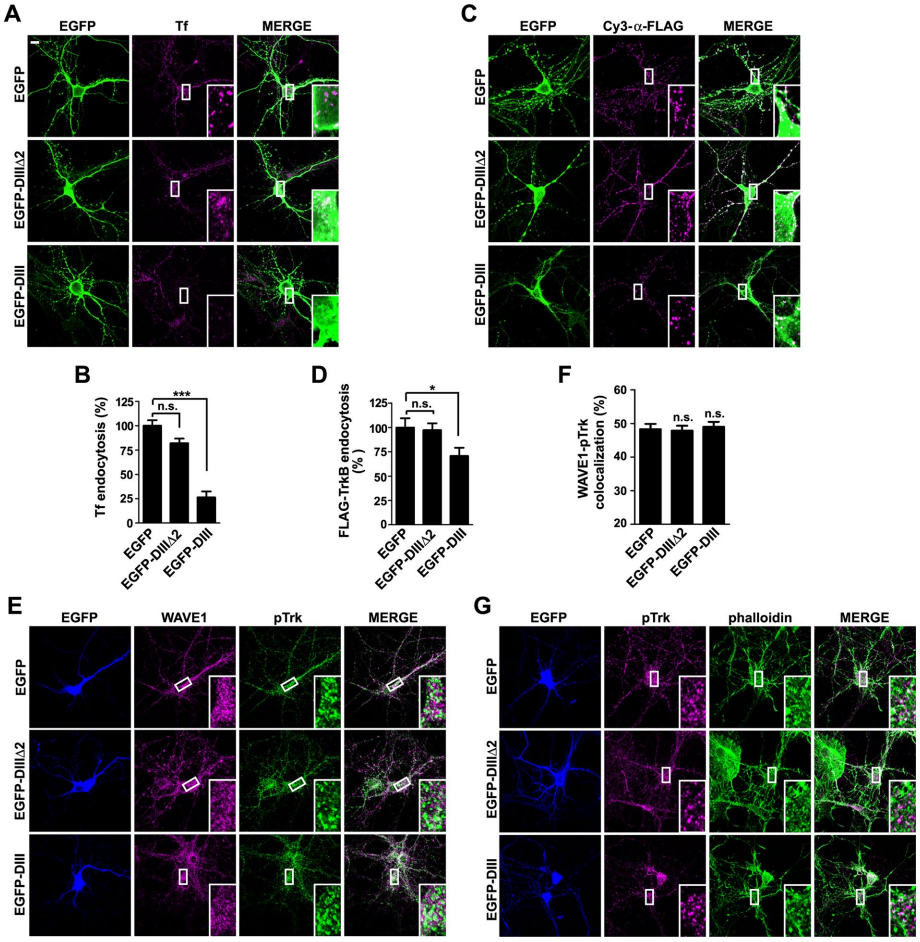

FIGURE 9: WAVE1-mediated endocytosis of BDNF-TrkB is not inhibited by overexpression of Eps15 dominant-negative mutant. (A) Hippocampal neurons were transfected with construct expressing EGFP, EGFP-Eps15 DIIIΔ2 (also known as EGFP-DIIIΔ2), or EGFP-Eps15 DIII (also known as EGFP-DIII) at DIV6, treated with 10 μg/ml Alexa Fluor 568–conjugated Tf for 15 min, washed with acid buffer, and fixed at DIV7. (B) Quantification of Tf endocytosis in neurons in A by measuring mean fluorescence intensity of Tf puncta per neuron (20–25 neurons from two independent experiments). EGFP-DIIIΔ2 serves as negative control for EGFP-DIII. (C) Hippocampal neurons cotransfected with expression constructs for FLAG-TrkB and EGFP, EGFP-DIIIΔ2, or EGFP-DIII at DIV6 were treated with BDNF (25 ng/ml) for 30 min at DIV7. Internalized FLAG-TrkB was labeled with Cy3–α-FLAG. (D) Quantification of Flag–TrkB endocytosis in neurons in C by measuring mean fluorescence intensity of FLAG-TrkB puncta per neuron (25 neurons from two independent experiments). (E) Hippocampal neurons transfected with construct expressing EGFP, EGFP-DIIIΔ2, or EGFP-DIII were starved for 2 h, stimulated with BDNF for 2 min, and immunostained with antibodies against WAVE1 and pTrk. (F) Quantification of the colocalization between WAVE1 and pTrk in E. Twenty neurons from two independent experiments were analyzed. (G) Same as E, except that neurons were stained with anti-pTrk and Alexa Fluor 568–conjugated phalloidin. Representative confocal images. Data represent mean ± SEM. *$p < 0.05$, ***$p < 0.001$. n.s., not significant. Scale bar, 10 μm.

rather than polymerization is essential for internalization of NGF-activated TrkA in distal axons of sympathetic neurons (Harrington *et al.*, 2011), in contrast to our findings that WAVE1-promoted actin polymerization is required for endocytosis of BDNF-activated TrkB in dendrites of CNS neurons. These seemingly contradictory findings suggest that a role for actin polymerization/depolymerization in trafficking of Trk family members in the highly polarized neuronal cells may also vary depending on cell type, type and site of endocytosis (e.g., axon vs. dendrite or soma), and receptor-specific modulators. Internalization of Trk receptor upon neurotrophin binding occurs via both clathrin-dependent and clathrin-independent pathways (Grimes *et al.*, 1997; Shao *et al.*, 2002; Valdez *et al.*, 2005, 2007; Zheng *et al.*, 2008). In the present study, we demonstrate that the majority of BDNF-activated TrkB endocytosis in the somatodendritic region of hippocampal neurons is clathrin independent. We also show that inhibition of CME does not affect recruitment of WAVE1 and accumulation of F-actin at endocytic sites of pTrk, indicating that WAVE1-mediated, actin-dependent endocytosis of TrkB is clathrin independent, which is in good agreement with recent findings on WAVE involvement in actin-dependent, clathrin-independent endocytosis of interleukin-2 receptor (Basquin *et al.*, 2015).

Stimulation of N-WASP during endocytosis is accomplished by the combination of upstream signals, including membrane lipids, Cdc42, and endophilin A (Prehoda *et al.*, 2000; Rohatgi *et al.*, 2000; Otsuki *et al.*, 2003). As a result, N-WASP integrates multiple upstream signals to target actin polymerization precisely to the endocytic site. In retrolinkin-mediated endocytosis of BDNF-TrkB, WAVE1 is recruited by retrolinkin through the CYFIP1/2 components of the WRC. It remains to be determined whether other factors, such as cargo adaptors, membrane lipids generated through pTrk-activated PI3K/Akt signaling pathways, components of the endocytic machinery, and/or any other unknown factors contribute to WAVE1 activation and association with receptor-clustered plasma membrane. It is conceivable that multiple weak interactions between WASP/WAVE family members and cellular factors ensure site specificity for subcellular localizations to achieve precise spatiotemporal control of actin filament network assembly in distinct cellular processes.

MATERIALS AND METHODS

Animal studies

The use of animals was approved by the Animal Care Committee of the Institute of Genetics and Developmental Biology, Chinese Academy of Sciences.

DNA constructs and shRNAs

pGEX4T-1-RTLN-N (aa 31–460) and pGEX4T-1-RTLN-C (aa 489–574) were constructed with mouse retrolinkin cDNA. RTLNΔC (aa 1–465) was inserted into pCDH-CMV-MCS-EF1-copGFP (System Biosciences, Mountain View, CA). RTLN-C1 (aa 496-574) was inserted into pEGFP-N2 (Clontech, Mountain View, CA). Mouse CYFIP2 and NAP1 cDNA were amplified from mouse brain cDNA obtained by reverse transcription (RT)-PCR and inserted into pcDNA3.1(+) and pCMV-Tag2B, respectively. pcDNA3.1(+)-CYFIP2, pcDNA3.1(+)-CYFIP2-N (aa 1–624), pcDNA3.1(+)-CYFIP2-C (aa 625–1253), and pET28a-CYFIP2-N (aa 1–624) were constructed with mouse CYFIP2 cDNA using standard molecular biology methods. The FLAG-WAVE1 expression construct was a generous gift from Lance Terada (UT Southwestern Medical Center, Dallas, TX). The

pCMV-Myc-WAVE1 construct was a generous gift from Yong Kim (Rockefeller University, New York, NY). The pRK5myc-Scar-W and -WA expression constructs were generous gifts from Laura Machesky (Glasgow University, Glasgow, United Kingdom). The Eps15 mutant constructs pEGFP-C2-DIIIΔ2 and pEGFP-C2-DIII were generous gifts from Alexandre Benmerah (INSERM, Institut Imagine, Paris, France). Myc-tagged, shRNA-resistant WAVE1 expression construct was generated by mutating AAGTAGCCTAAGTAAATAT (nucleotides [nt] 123–141 of human WAVE1-coding region) to AAGTAGCCTATCTAAATAT by site-directed mutagenesis. The shRNA-resistant retrolinkin expression construct was generated by mutating ACAACCTGAGCTACTGGAA (nt 1505–1523 of retrolinkin coding region) to ACAACCTGTCCTACTGGAA without changing the amino acid sequence.

To prepare shRNA constructs, each shRNA contained a 19-nt target sequence, the sense and antisense strands were annealed, and then the annealing oligos were inserted into pLentiLox 3.7 between the *Xho*I and *Hpa*I sites. All constructs were verified by sequencing. Target sequences for mouse retrolinkin shRNA (nt 1505–1523) were described previously (Fu *et al*., 2011).

Target sequences for mouse CYFIP1 shRNA (nt 2177–2195): 5′-GGTTACGGTCAGAATGCAA-3′; for mouse CYFIP2 shRNA #1 (nt 363–381): 5′-GCTCATGAAGTTCATGTAC-3′; for mouse CYFIP2 shRNA #2 (nt 2940–2958): 5′-GGACATCATCGAGTATGCA-3′; for mouse WAVE1 shRNA (nt 123–141): 5′-GAGTAGCCTAAGTAAGTAT-3′; for mouse N-WASP shRNA#1 (nt 178–196): 5′-GGTGTCGCTTGTCTGGTTA-3′; mouse N-WASP shRNA#2 (nt 325–343): 5′-GGAGATACTTGTCAAGTAG-3′; and for nontargeting control shRNA, which has no homology to known gene sequences: 5′-GAATGCTCTTACGATGATA-3′. All shRNA expression constructs were tested for knockdown efficiency. CYFIP2 shRNA #2 and N-WASP shRNA #2 were used for knockdown of CYFIP2 and N-WASP, respectively.

Antibodies and reagents

Rabbit and guinea pig polyclonal antibodies against mouse retrolinkin were prepared as described previously (Liu *et al*., 2007). Rabbit anti-CYFIP2 (peptide antigen CPFTQEPQRDKPANVQPY) and rabbit anti-NAP1 (peptide antigen CHAVYKQSVTSSA) were produced by Medical & Biological Laboratories (Naka-ku Nagoya, Japan). Antibodies used include rabbit polyclonal antibody against phospho-Trk (Tyr-490), rabbit anti-ERK1/2, mouse anti–phospho-ERK1/2 (Thr-202/Tyr-204), rabbit anti-Akt, rabbit anti–phospho-Akt (Ser-473), rabbit anti–N-WASP (Cell Signaling Technology, Beverly, MA), rabbit polyclonal antibody against phospho-Trk (Tyr-490; GeneTex, Irvine, CA), rabbit anti–pan-Trk, rabbit anti-TrkB, mouse anti-Myc (Santa Cruz Biotechnology, Santa Cruz, CA), rabbit anti-Myc, rabbit and mouse anti-GFP, rabbit and mouse anti-RFP, which recognizes DsRed and mCherry (Medical & Biological Laboratories); mouse anti–β-actin, mouse anti–FLAG M2-FITC, mouse anti–FLAG M2-Cy3 (Sigma-Aldrich, St. Louis, MO), mouse-anti-WAVE1, mouse anti-CYFIP1 (EMD Millipore, Billerica, MA), and rabbit anti-WAVE1 (Abcam, Cambridge, United Kingdom). Secondary antibodies for immunofluorescence staining were from Molecular Probes (Invitrogen, Carlsbad, CA). Dimethyl sulfoxide (DMSO) and latrunculin A were from Sigma-Aldrich (St. Louis, MO). CK-666 was obtained from EMD Millipore. Alexa Fluor 488– and Alexa Fluor 568–conjugated transferrin and Alexa Fluor 568– and Alexa Fluor 488–conjugated phalloidin were obtained from Thermo Fisher Scientific (Waltham, MA). Chlorpromazine was purchased from Target Molecule Corp. (TargetMol, Boston, MA), and Pitstop2 was from Abcam.

GST pull-down assays and mass spectrometry analysis

GST pull-down assays were performed as described previously (Fu *et al*., 2011). Briefly, GST-fused RTLN-N and RTLN-C were expressed and purified from *E. coli*. CYFIP2, NAP1, or WAVE1 constructs were expressed in HEK 293T cells for 48 h, and lysates were prepared in a buffer (50 mM Tris-HCl, pH 7.5, 150 mM NaCl, 1% NP-40) plus protease inhibitors. Cell lysates were centrifuged at 12,000 × *g* for 15 min at 4°C, and the supernatant was incubated with individual GST-fused proteins immobilized on glutathione–Sepharose beads for 2 h at room temperature. Beads were washed five times with a buffer containing 20 mM Tris-HCl, pH 7.5, 150 mM NaCl, and 0.1% Triton X-100 and boiled in SDS–PAGE sample buffer (100 mM Tris-Cl, pH 6.8, 4% SDS, 0.2% bromophenol blue, 20% [vol/vol] glycerol, 10% [vol/vol] 2-mercaptoethanol). Bound proteins were analyzed by SDS–PAGE and immunoblotting. For GST pull down from mouse brain lysates, adult mouse brain was homogenized in cold homogenization buffer (50 mM Tris-Cl, pH 7.4, 20 mM 4-(2-hydroxyethyl)-1-piperazineethanesulfonic acid, pH 7.4, 150 mM NaCl, 1% NP-40, 1 mM phenylmethylsulfonyl fluoride [PMSF], and 1× protease inhibitors). Lysates were centrifuged at 12,000 × *g* for 15 min at 4°C, and the supernatants were incubated with GST fusion protein conjugated with glutathione–Sepharose beads overnight at 4°C. For mass spectrometry analysis of bound proteins, beads were boiled with 2× SDS sample buffer, and the protein samples were subjected to SDS–PAGE. The silver-stained protein bands were excised from the gel and subjected to in-gel digestion with trypsin and mass spectrometry analysis. For in vitro binding assay, histidine (His)-tagged CYFIP2-N was purified from *E. coli* with Ni–nitriloacetic acid resin (EMD Millipore) for 2 h at 4°C with gentle rotation. A 10-µg amount of GST-tagged retrolinkin conjugated with glutathione–Sepharose beads was incubated with 3 µg of His-tagged CYFIP2-N in binding buffer (20 mM Tris-HCl, pH 7.5, 150 mM NaCl, 5 mM EDTA, 1% NP-40, and bovine serum albumin [BSA; 25 mg/ml]) at 4°C overnight. Beads were washed five times with binding buffer, and bound proteins were eluted from the beads in 2× SDS sample buffer and subjected to SDS–PAGE and immunoblotting.

Immunoprecipitation

Adult mouse brain or HEK 293T cells were homogenized in 1 ml of cold homogenization buffer, and the homogenates were centrifuged at 12,000 × *g* for 15 min at 4°C. For FLAG-IP, supernatants were incubated with anti-FLAG Affinity Gel (Sigma-Aldrich) overnight at 4°C. For other IPs, the supernatants were incubated with antibodies (2–5 µg) at 4°C for 2 h, followed by incubation with 25 µl of Protein A/G–Sepharose (Santa Cruz Biotechnology) preequilibrated in lysis buffer overnight at 4°C. Precipitates were washed five times with ice-cold TBS (50 mM Tris-Cl, pH 7.4, 150 mM NaCl, 0.1% Triton X-100). Bound proteins were eluted from the beads in 2× SDS sample buffer and subjected to SDS–PAGE and immunoblotting. Membrane IP was performed with the membrane fractions (P100) of brain lysates after ultracentrifugation at 100,000 × *g* for 1 h. After ultracentrifugation, the pellets were resuspended with lysis buffer (50 mM Tris-HCl, pH 7.5, 150 mM NaCl, 1% NP-40) and incubated with antibodies (2–5 µg) and 25 µl of Protein A/G Sepharose (Santa Cruz Biotechnology) at 4°C. After overnight incubation of membranes with beads, the beads were washed with ice-cold TBS five times, and bound proteins were eluted from the beads in 2× SDS sample buffer and subjected to SDS–PAGE and immunoblotting.

Cell culture, transfection, and viral infection

HEK 293T and HEK 293 cells were cultured in DMEM supplemented with 10% fetal bovine serum. Transfections were performed using

VigoFect (Vigorous Biotechnology, Beijing, China) according to manufacturer's instructions. Cells were harvested 24–48 h after transfection.

Primary neuronal cultures from mouse hippocampi or cortex were prepared as described previously (Banker and Goslin, 1988). Briefly, hippocampi and cortex were dissected from embryonic day 16.5 (E16.5) BALB/c mouse, dissociated with 0.25% trypsin in Hanks' balanced salt solution without Ca^{2+} and Mg^{2+} at 37°C for 15 min, and triturated in DMEM, 10% F-12, and 10% fetal bovine serum. Hippocampal neurons were plated on coverslips coated with poly-D-lysine (0.1 mg/ml) in 24-well plates at a density of 1×10^5 cells/well. Cortical neurons were plated on six- or 12-well plates coated with poly-D-lysine (0.1 mg/ml) at a density of 5×10^5 or 1×10^6 cells/well. The medium was changed to the serum-free medium (Neurobasal Medium supplemented with B27 supplement [2%], GlutaMAX [1%], Fungizone [1:500], and gentamicin [1:1000]) 4 h after plating. For neuronal morphology and immunostaining analyses, neurons were transfected with Lipofectamine 2000 (Invitrogen) following the manufacturer's instructions. Briefly, DNA (1.2 μg/well) was mixed with 1 μl of Lipofectamine 2000 in 250 μl of Neurobasal Medium, incubated for 20 min, and then added to neurons in 250 μl of Neurobasal Medium at 37°C in 5% CO_2 for 1 h. Neurons were then incubated in the original medium at 37°C in 5% CO_2 for 3–5 d. For Western blotting, neurons were infected with lentivirus prepared from HEK293T cells (Yang *et al.*, 2015) for 6–8 h at DIV3–4, Neurons were then rinsed with Neurobasal Medium, transferred to the original medium at 37°C in 5% CO_2 , and harvested after 6–7 d.

Immunofluorescence staining, image acquisition, and analysis

Hippocampal neurons were fixed in 4% paraformaldehyde (PFA)/4% sucrose in phosphate-buffered saline (PBS) for 15 min at room temperature and then permeabilized in 0.4% Triton X-100 in PBS for 10 min at room temperature. After blocking with 1% BSA in PBS containing 0.4% Triton X-100 for 1 h at room temperature, neurons were incubated with primary antibodies for 2 h at room temperature or overnight at 4°C, and appropriate secondary antibodies conjugated with Alexa Fluor 488, Alexa Fluor 555, or Alexa Fluor 647 were used for detection. Confocal images were collected using the Spectral Imaging Confocal Microscope Digital Eclipse C1Si (Nikon, Tokyo, Japan) with a 100× Plan Apochromat VC numerical aperture 1.40 oil objective.

Quantification of the colocalization between pTrk and WAVE1 in neurons was performed as described previously (Fu *et al.*, 2011). The colocalization of the pTrk and WAVE1 fluorescence signals was calculated as the Mander's overlap coefficient with the NIS-Elements AR software (Nikon). Values for colocalization analysis represent mean value ± SEM. For quantitative analyses of BDNF-stimulated TrkB endocytosis and transferrin uptake, we drew out the region of interest (ROI) of transfected neurons according to the volume marker and then measured mean fluorescence intensity of the fluorescent puncta superimposed on an unspecific background with the NIS-Elements AR software. For quantification of FLAG-TrkB surface level and transferrin binding to the plasma membrane, we drew out the cell body area and three dendritic segments (15 μm/segment) as ROI of transfected neurons and measured mean fluorescence intensity.

Sholl analysis

A modified Sholl analysis was performed with the Sholl analysis plugin of ImageJ (National Institutes of Health, Bethesda, MD) as described (Whitford *et al.*, 2002). In brief, the center of the soma was selected as the center of all of the circles to be analyzed. The concentric circles were drawn from 10 to 100 μm by 5-μm-step intervals. The number of circles was chosen to cover the entire dendrite from soma to tips. A series of concentric circles was centered on the cell body, and the number of processes crossing each of the circles was counted. Between 30 and 35 neurons per condition were quantified, and the results at each interval were compared by an unpaired Student's *t* test.

Quantification of neurite length and soma size

In the morphological study of hippocampal neurons, the length of axon and dendrite and the soma area were measured with NIS-Elements AR. Total dendritic branch length (TDBL) is the sum of the lengths of all dendrites. Primary dendrite lengths were excluded from the total dendritic branch tip length. Axons were excluded from the dendrites by their distinct morphology (Cheadle and Biederer, 2014).

TrkB internalization assay and transferrin uptake assay

TrkB internalization assay was performed as described previously (Sharma *et al.*, 2010; Fu *et al.*, 2011). Briefly, DIV3 hippocampal neurons were cotransfected with the FLAG-TrkB and shRNA expression constructs. After starvation with MEM for 2 h on DIV7, neurons were incubated with FITC–anti-FLAG antibody (5 μg/ml; Sigma-Aldrich) for 30 min at room temperature to label FLAG-tagged TrkB receptors on the plasma membrane. Cells were rinsed with MEM twice to remove unbound antibodies and then incubated with BDNF (25 ng/ml) for 30 min at 37°C, followed by two quick washes with acid buffer (500 mM NaCl, 200 mM acetic acid) to remove surface-bound fluorescent antibodies. Cells were then fixed with 4% PFA and analyzed by confocal microscopy, with the intracellular fluorescence representing the internalized receptors.

Transferrin (Tf) uptake assay was performed basically as described previously (Fu *et al.*, 2011), except that neurons were incubated with Alexa Fluor 488– or Alexa Fluor 568–conjugated Tf for 15 min at 37°C followed by two quick washes with acid buffer to remove surface-bound Tf.

Biotinylation assay of surface TrkB

Biotinylation assay of surface TrkB was performed as described (Wan *et al.*, 2008; Fu *et al.*, 2011).

BDNF signaling assays

Primary mouse cortical neurons were infected with lentivirus expressing shRNA on DIV3 and cultured for 7 d. DIV10 neurons were starved for 2 h with MEM supplemented with 20 μg/ml cycloheximide, followed by incubation with BDNF (25 ng/ml) in MEM for 15, 30, or 60 min. Cells were then washed once with ice-cold PBS and lysed in lysis buffer (50 mM Tris-Cl, pH 7.4, 150 mM NaCl, 1% Triton X-100, 1 mM Na_3VO_4, 10 mM NaF, 1 mM PMSF). After centrifugation at 12,000 × *g* at 4°C for 10 min, the supernatant was boiled with SDS sample buffer and subjected to SDS–PAGE and immunoblotting. The immunoblots were probed with antibodies against Erk1/2, pErk, Akt, and pAkt.

Drug treatment and phalloidin staining

For inhibition of actin polymerization, neurons were starved with MEM for 1 h. Latrunculin A dissolved in DMSO was diluted with MEM and added to neurons at a final concentration of 1 μM for 1 h. For inhibition of Arp2/3 activity, neurons were starved with MEM for 2 h. CK-666 dissolved in DMSO was diluted with MEM and added to neurons at a final concentration of 200 μM for 2 h. For F-actin

staining, Alexa Fluor 488– or Alexa Fluor 568–conjugated phalloidin diluted with PBS (1:200) was incubated with neurons for 1 h at room temperature.

Statistical analysis

All data are presented as mean ± SEM. GraphPad Prism 5 (GraphPad Software, La Jolla, CA) was used for statistical analysis. For two-sample comparisons versus controls, the two-tailed unpaired Student's *t* test was used. One-way analysis of variance (ANOVA) with a Dunnett's multiple-comparison was used to evaluate statistical significance of three or more groups of samples. $p < 0.05$ was considered statistically significant.

ACKNOWLEDGMENTS

We thank Lance Terada, Yong Kim, Laura Machesky, and Alexandre Benmerah for generously providing us with reagents; Yuhang Chen (Institute of Genetics and Developmental Biology, Chinese Academy of Sciences) for technical advice on recombinant protein expression; and the Research Centre for Life Sciences, University of Science and Technology of China, and Institute of Biophysics, Chinese Academy of Sciences, for mass spectrometry analysis. We also thank the members of the Liu lab for helpful discussions and comments on the manuscript. This work was supported by the National Natural Science Foundation of China (31530039, 31471334, and 31325017) and the Ministry of Science and Technology of China (2014CB942802 and 2016YFA0500100).

REFERENCES

Banker G, Goslin K (1988). Developments in neuronal cell culture. Nature 336, 185–186.

Basquin C, Trichet M, Vihinen H, Malarde V, Lagache T, Ripoll L, Jokitalo E, Olivo-Marin JC, Gautreau A, Sauvonnet N (2015). Membrane protrusion powers clathrin-independent endocytosis of interleukin-2 receptor. EMBO J 34, 2147–2161.

Beattie EC, Howe CL, Wilde A, Brodsky FM, Mobley WC (2000). NGF signals through TrkA to increase clathrin at the plasma membrane and enhance clathrin-mediated membrane trafficking. J Neurosci 20, 7325–7333.

Benesch S, Polo S, Lai FP, Anderson KI, Stradal TE, Wehland J, Rottner K (2005). N-WASP deficiency impairs EGF internalization and actin assembly at clathrin-coated pits. J Cell Sci 118, 3103–3115.

Benmerah A, Bayrou M, Cerf-Bensussan N, Dautry-Varsat A (1999). Inhibition of clathrin-coated pit assembly by an Eps15 mutant. J Cell Sci 112, 1303–1311.

Benmerah A, Lamaze C, Begue B, Schmid SL, Dautry-Varsat A, Cerf-Bensussan N (1998). AP-2/Eps15 interaction is required for receptor-mediated endocytosis. J Cell Biol 140, 1055–1062.

Benmerah A, Poupon V, Cerf-Bensussan N, Dautry-Varsat A (2000). Mapping of Eps15 domains involved in its targeting to clathrin-coated pits. J Biol Chem 275, 3288–3295.

Cheadle L, Biederer T (2014). Activity-dependent regulation of dendritic complexity by semaphorin 3A through Farp1. J Neurosci 34, 7999–8009.

Chen B, Brinkmann K, Chen Z, Pak CW, Liao Y, Shi S, Henry L, Grishin NV, Bogdan S, Rosen MK (2014). The WAVE regulatory complex links diverse receptors to the actin cytoskeleton. Cell 156, 195–207.

Chen Z, Borek D, Padrick SB, Gomez TS, Metlagel Z, Ismail AM, Umetani J, Billadeau DD, Otwinowski Z, Rosen MK (2010). Structure and control of the actin regulatory WAVE complex. Nature 468, 533–538.

Chen ZY, Ieraci A, Tanowitz M, Lee FS (2005). A novel endocytic recycling signal distinguishes biological responses of Trk neurotrophin receptors. Mol Biol Cell 16, 5761–5772.

Cosker KE, Segal RA (2014). Neuronal signaling through endocytosis. Cold Spring Harb Perspect Biol 6, a020669.

Coue M, Brenner SL, Spector I, Korn ED (1987). Inhibition of actin polymerization by latrunculin A. FEBS Lett 213, 316–318.

Dahl JP, Wang-Dunlop J, Gonzales C, Goad ME, Mark RJ, Kwak SP (2003). Characterization of the WAVE1 knock-out mouse: implications for CNS development. J Neurosci 23, 3343–3352.

Delcroix JD, Valletta JS, Wu C, Hunt SJ, Kowal AS, Mobley WC (2003). NGF signaling in sensory neurons: evidence that early endosomes carry NGF retrograde signals. Neuron 39, 69–84.

Derivery E, Gautreau A (2010). Generation of branched actin networks: assembly and regulation of the N-WASP and WAVE molecular machines. Bioessays 32, 119–131.

Eden S, Rohatgi R, Podtelejnikov AV, Mann M, Kirschner MW (2002). Mechanism of regulation of WAVE1-induced actin nucleation by Rac1 and Nck. Nature 418, 790–793.

Fu X, Yang Y, Xu C, Niu Y, Chen T, Zhou Q, Liu JJ (2011). Retrolinkin cooperates with endophilin A1 to mediate BDNF-TrkB early endocytic trafficking and signaling from early endosomes. Mol Biol Cell 22, 3684–3698.

Grimes ML, Beattie E, Mobley WC (1997). A signaling organelle containing the nerve growth factor-activated receptor tyrosine kinase, TrkA. Proc Natl Acad Sci USA 94, 9909–9914.

Harrington AW, St Hillaire C, Zweifel LS, Glebova NO, Philippidou P, Halegoua S, Ginty DD (2011). Recruitment of actin modifiers to TrkA endosomes governs retrograde NGF signaling and survival. Cell 146, 421–434.

Howe CL, Valletta JS, Rusnak AS, Mobley WC (2001). NGF signaling from clathrin-coated vesicles: evidence that signaling endosomes serve as a platform for the Ras-MAPK pathway. Neuron 32, 801–814.

Huang EJ, Reichardt LF (2003). Trk receptors: roles in neuronal signal transduction. Annu Rev Biochem 72, 609–642.

Innocenti M, Gerboth S, Rottner K, Lai FP, Hertzog M, Stradal TE, Frittoli E, Didry D, Polo S, Disanza A, *et al.* (2005). Abi1 regulates the activity of N-WASP and WAVE in distinct actin-based processes. Nat Cell Biol 7, 969–976.

Irie F, Yamaguchi Y (2002). EphB receptors regulate dendritic spine development via intersectin, Cdc42 and N-WASP. Nat Neurosci 5, 1117–1118.

Kaplan DR, Miller FD (2000). Neurotrophin signal transduction in the nervous system. Curr Opin Neurobiol 10, 381–391.

Kessels MM, Qualmann B (2002). Syndapins integrate N-WASP in receptor-mediated endocytosis. EMBO J 21, 6083–6094.

Kim Y, Sung JY, Ceglia I, Lee KW, Ahn JH, Halford JM, Kim AM, Kwak SP, Park JB, Ho Ryu S, *et al.* (2006). Phosphorylation of WAVE1 regulates actin polymerization and dendritic spine morphology. Nature 442, 814–817.

Koronakis V, Hume PJ, Humphreys D, Liu T, Horning O, Jensen ON, McGhie EJ (2011). WAVE regulatory complex activation by cooperating GTPases Arf and Rac1. Proc Natl Acad Sci USA 108, 14449–14454.

Lebensohn AM, Kirschner MW (2009). Activation of the WAVE complex by coincident signals controls actin assembly. Mol Cell 36, 512–524.

Liu JJ, Ding J, Wu C, Bhagavatula P, Cui B, Chu S, Mobley WC, Yang Y (2007). Retrolinkin, a membrane protein, plays an important role in retrograde axonal transport. Proc Natl Acad Sci USA 104, 2223–2228.

Liu XH, Geng Z, Yan J, Li T, Chen Q, Zhang QY, Chen ZY (2015). Blocking GSK3beta-mediated dynamin1 phosphorylation enhances BDNF-dependent TrkB endocytosis and the protective effects of BDNF in neuronal and mouse models of Alzheimer's disease. Neurobiol Dis 74, 377–391.

Machesky LM, Insall RH (1998). Scar1 and the related Wiskott-Aldrich syndrome protein, WASP, regulate the actin cytoskeleton through the Arp2/3 complex. Curr Biol 8, 1347–1356.

Merrifield CJ, Perrais D, Zenisek D (2005). Coupling between clathrin-coated-pit invagination, cortactin recruitment, and membrane scission observed in live cells. Cell 121, 593–606.

Merrifield CJ, Qualmann B, Kessels MM, Almers W (2004). Neural Wiskott Aldrich Syndrome Protein (N-WASP) and the Arp2/3 complex are recruited to sites of clathrin-mediated endocytosis in cultured fibroblasts. Eur J Cell Biol 83, 13–18.

Mettlen M, Stoeber M, Loerke D, Antonescu CN, Danuser G, Schmid SL (2009). Endocytic accessory proteins are functionally distinguished by their differential effects on the maturation of clathrin-coated pits. Mol Biol Cell 20, 3251–3260.

Mooren OL, Galletta BJ, Cooper JA (2012). Roles for actin assembly in endocytosis. Annu Rev Biochem 81, 661–686.

Namekata K, Harada C, Taya C, Guo X, Kimura H, Parada LF, Harada T (2010). Dock3 induces axonal outgrowth by stimulating membrane recruitment of the WAVE complex. Proc Natl Acad Sci USA 107, 7586–7591.

Nolen BJ, Tomasevic N, Russell A, Pierce DW, Jia Z, McCormick CD, Hartman J, Sakowicz R, Pollard TD (2009). Characterization of two classes of small molecule inhibitors of Arp2/3 complex. Nature 460, 1031–1034.

Nozumi M, Nakagawa H, Miki H, Takenawa T, Miyamoto S (2003). Differential localization of WAVE isoforms in filopodia and lamellipodia of the neuronal growth cone. J Cell Sci 116, 239–246.

Oikawa T, Yamaguchi H, Itoh T, Kato M, Ijuin T, Yamazaki D, Suetsugu S, Takenawa T (2004). PtdIns(3,4,5)P3 binding is necessary for WAVE2-induced formation of lamellipodia. Nat Cell Biol 6, 420–426.

Otsuki M, Itoh T, Takenawa T (2003). Neural Wiskott-Aldrich syndrome protein is recruited to rafts and associates with endophilin A in response to epidermal growth factor. J Biol Chem 278, 6461–6469.

Prehoda KE, Scott JA, Mullins RD, Lim WA (2000). Integration of multiple signals through cooperative regulation of the N-WASP-Arp2/3 complex. Science 290, 801–806.

Rohatgi R, Ho HY, Kirschner MW (2000). Mechanism of N-WASP activation by CDC42 and phosphatidylinositol 4, 5-bisphosphate. J Cell Biol 150, 1299–1310.

Segal RA (2003). Selectivity in neurotrophin signaling: theme and variations. Annu Rev Neurosci 26, 299–330.

Shao Y, Akmentin W, Toledo-Aral JJ, Rosenbaum J, Valdez G, Cabot JB, Hilbush BS, Halegoua S (2002). Pincher, a pinocytic chaperone for nerve growth factor/TrkA signaling endosomes. J Cell Biol 157, 679–691.

Sharma N, Deppmann CD, Harrington AW, St Hillaire C, Chen ZY, Lee FS, Ginty DD (2010). Long-distance control of synapse assembly by target-derived NGF. Neuron 67, 422–434.

Shekarabi M, Moore SW, Tritsch NX, Morris SJ, Bouchard JF, Kennedy TE (2005). Deleted in colorectal cancer binding netrin-1 mediates cell substrate adhesion and recruits Cdc42, Rac1, Pak1, and N-WASP into an intracellular signaling complex that promotes growth cone expansion. J Neurosci 25, 3132–3141.

Shin N, Lee S, Ahn N, Kim SA, Ahn SG, YongPark Z, Chang S (2007). Sorting nexin 9 interacts with dynamin 1 and N-WASP and coordinates synaptic vesicle endocytosis. J Biol Chem 282, 28939–28950.

Soderling SH, Guire ES, Kaech S, White J, Zhang F, Schutz K, Langeberg LK, Banker G, Raber J, Scott JD (2007). A WAVE-1 and WRP signaling complex regulates spine density, synaptic plasticity, and memory. J Neurosci 27, 355–365.

Soderling SH, Langeberg LK, Soderling JA, Davee SM, Simerly R, Raber J, Scott JD (2003). Loss of WAVE-1 causes sensorimotor retardation and reduced learning and memory in mice. Proc Natl Acad Sci USA 100, 1723–1728.

Spector I, Shochet NR, Blasberger D, Kashman Y (1989). Latrunculins–novel marine macrolides that disrupt microfilament organization and affect cell growth: I. Comparison with cytochalasin D. Cell Motil Cytoskeleton 13, 127–144.

Suetsugu S, Kurisu S, Oikawa T, Yamazaki D, Oda A, Takenawa T (2006). Optimization of WAVE2 complex-induced actin polymerization by membrane-bound IRSp53, PIP(3), and Rac. J Cell Biol 173, 571–585.

Suetsugu S, Yamazaki D, Kurisu S, Takenawa T (2003). Differential roles of WAVE1 and WAVE2 in dorsal and peripheral ruffle formation for fibroblast cell migration. Dev Cell 5, 595–609.

Valdez G, Akmentin W, Philippidou P, Kuruvilla R, Ginty DD, Halegoua S (2005). Pincher-mediated macroendocytosis underlies retrograde signaling by neurotrophin receptors. J Neurosci 25, 5236–5247.

Valdez G, Philippidou P, Rosenbaum J, Akmentin W, Shao Y, Halegoua S (2007). Trk-signaling endosomes are generated by Rac-dependent macroendocytosis. Proc Natl Acad Sci USA 104, 12270–12275.

von Kleist L, Stahlschmidt W, Bulut H, Gromova K, Puchkov D, Robertson MJ, MacGregor KA, Tomilin N, Pechstein A, Chau N, Chircop M, *et al.* (2011). Role of the clathrin terminal domain in regulating coated pit dynamics revealed by small molecule inhibition. Cell 146, 471–484.

Wan J, Cheung AY, Fu WY, Wu C, Zhang M, Mobley WC, Cheung ZH, Ip NY (2008). Endophilin B1 as a novel regulator of nerve growth factor/ TrkA trafficking and neurite outgrowth. J Neurosci 28, 9002–9012.

Wang LH, Rothberg KG, Anderson RG (1993). Mis-assembly of clathrin lattices on endosomes reveals a regulatory switch for coated pit formation. J Cell Biol 123, 1107–1117.

Whitford KL, Marillat V, Stein E, Goodman CS, Tessier-Lavigne M, Chedotal A, Ghosh A (2002). Regulation of cortical dendrite development by Slit-Robo interactions. Neuron 33, 47–61.

Wulf E, Deboben A, Bautz FA, Faulstich H, Wieland T (1979). Fluorescent phallotoxin, a tool for the visualization of cellular actin. Proc Natl Acad Sci USA 76, 4498–4502.

Yang Y, Wei M, Xiong Y, Du X, Zhu S, Yang L, Zhang C, Liu JJ (2015). Endophilin A1 regulates dendritic spine morphogenesis and stability through interaction with p140Cap. Cell Res 25, 496–516.

Yarar D, Waterman-Storer CM, Schmid SL (2007). SNX9 couples actin assembly to phosphoinositide signals and is required for membrane remodeling during endocytosis. Dev Cell 13, 43–56.

Zheng J, Shen WH, Lu TJ, Zhou Y, Chen Q, Wang Z, Xiang T, Zhu YC, Zhang C, Duan S, Xiong ZQ (2008). Clathrin-dependent endocytosis is required for TrkB-dependent Akt-mediated neuronal protection and dendritic growth. J Biol Chem 283, 13280–13288.

Zhou P, Alfaro J, Chang EH, Zhao X, Porcionatto M, Segal RA (2011). Numb links extracellular cues to intracellular polarity machinery to promote chemotaxis. Dev Cell 20, 610–622.